White Matter Diseases with Radiologic-Pathologic Correlation[1]

Nicolae Sarbu, MD
Robert Y. Shih, MD
Robert V. Jones, MD
Iren Horkayne-Szakaly, MD
Laura Oleaga, MD, PhD
James G. Smirniotopoulos, MD

Abbreviations: ADEM = acute disseminated encephalomyelitis, CADASIL = cerebral autosomal-dominant arteriopathy with subcortical infarcts and leukoencephalopathy, FLAIR = fluid-attenuated inversion-recovery, HIV = human immunodeficiency virus, MS = multiple sclerosis, NMO = neuromyelitis optica, PACNS = primary angiitis of the central nervous system, PML = progressive multifocal leukoencephalopathy, PRES = posterior reversible encephalopathy syndrome, SLE = systemic lupus erythematosus, TDL = tumefactive demyelinating lesion, WMH = white matter hyperintensity

RadioGraphics 2016; 36:1426–1447

Published online 10.1148/rg.2016160031

Content Codes: MR NR

[1]From the Department of Radiology, Hospital Clínic Barcelona, Barcelona, Spain (N.S., L.O.); and American Institute for Radiologic Pathology, Silver Spring, Md (R.Y.S., R.V.J., I.H.S., J.G.S.). Presented as an education exhibit at the 2015 RSNA Annual Meeting. Received February 27, 2016; revision requested April 22 and received May 14; accepted May 25. For this journal-based SA-CME activity, the authors, editor, and reviewers have disclosed no relevant relationships. **Address correspondence to** J.G.S., Professorial Lecturer, George Washington University, 204 Eldrid Dr, Silver Spring, MD 20904 (e-mail: *medpixman@gmail.com*).

N.S. supported by a 3-month academic scholarship (2014) to the American Institute for Radiologic Pathology from the Fundación Española de Radiología–Sociedad Española de Radiología de Radiología Médica (FER-SERAM).

SA-CME LEARNING OBJECTIVES

After completing this journal-based SA-CME activity, participants will be able to:

- Recognize the imaging appearances of white matter diseases.
- Describe the histologic substrate of white matter diseases.
- Discuss the key differentiating features between different white matter diseases.

See www.rsna.org/education/search/RG.

White matter diseases include a wide spectrum of disorders that have in common impairment of normal myelination, either by secondary destruction of previously myelinated structures (demyelinating processes) or by primary abnormalities of myelin formation (dysmyelinating processes). The pathogenesis of many white matter diseases remains poorly understood. Demyelinating disorders are the object of this review and will be further divided into autoimmune, infectious, vascular, and toxic-metabolic processes. Autoimmune processes include multiple sclerosis and related diseases: tumefactive demyelinating lesions, Balo concentric sclerosis, Marburg and Schilder variants, neuromyelitis optica (Devic disease), acute disseminated encephalomyelitis, and acute hemorrhagic leukoencephalopathy (Hurst disease). Infectious processes include Lyme disease (neuroborreliosis), progressive multifocal leukoencephalopathy, and human immunodeficiency virus (HIV) encephalopathy. Vascular processes include different types of small-vessel disease: arteriolosclerosis, cerebral amyloid angiopathy, cerebral autosomal-dominant arteriopathy with subcortical infarcts and leukoencephalopathy (CADASIL), primary angiitis of the central nervous system, Susac syndrome, and neurolupus. Toxic-metabolic processes include osmotic myelinolysis, methotrexate leukoencephalopathy, and posterior reversible encephalopathy syndrome. The imaging spectrum can vary widely from small multifocal white matter lesions to confluent or extensive white matter involvement. Understanding the pathologic substrate is fundamental for understanding the radiologic manifestations, and a systematic approach to the radiologic findings, in correlation with clinical and laboratory data, is crucial for narrowing the differential diagnosis.

Introduction

White matter diseases affect the pattern of normal myelination and include a large diversity of congenital and acquired processes. They can be divided into demyelinating (secondary destruction of normal myelin) or dysmyelinating (primary abnormality of myelin formation) processes. Demyelinating diseases can be further divided into autoimmune, infectious, vascular, and toxic-metabolic categories.

Demyelinating processes are commonly separated into primary and secondary types according to their cause. Primary demyelinating disorders are of (currently) unknown etiology, and their prototype is multiple sclerosis (MS). Secondary demyelinating diseases include a variety of known causes. Independent of their cause, the underlying condition of all demyelinating disorders is damage to the myelin or to the cells that produce the myelin, the oligodendrocytes (1). This review explores the clinicopathophysiology of white matter demyelinating disorders using radiologic-pathologic correlation.

TEACHING POINTS

- White matter diseases affect the pattern of normal myelination and include a large diversity of congenital and acquired processes. They can be divided into demyelinating (secondary destruction of normal myelin) or dysmyelinating (primary abnormality of myelin formation) processes. Demyelinating diseases can be further divided into autoimmune, infectious, vascular, and toxic-metabolic categories.
- MS is a primary demyelinating disease of unknown etiology (autoimmune category), characterized by perivenular inflammation/demyelination with relative axon preservation, manifesting as periventricular, juxtacortical, infratentorial, and spinal cord lesions at magnetic resonance (MR) imaging.
- TDLs can be mistaken for high-grade enhancing neoplasms—possible clues to the diagnosis include an incomplete ring of enhancement and/or restricted diffusion reflecting the advancing front of demyelination, a paucity of perilesional edema, relative lack of mass effect for lesion size, and lower cerebral blood volume at perfusion imaging.
- HIV encephalopathy shares some features with PML: both cause confluent white matter lesions without significant mass effect or enhancement, but more peripheral and asymmetric in PML (infecting oligodendrocytes) versus more central and symmetric in HIV encephalopathy (infecting microglia).
- Small-vessel disease is by far the leading cause of white matter disease and can be divided into six types: arteriolosclerosis (type 1); cerebral amyloid angiopathy (type 2); inherited vasculopathies (type 3) (eg, CADASIL, MELAS [*m*itochondrial myopathy, *e*ncephalopathy, *l*actic *a*cidosis, *s*trokelike episodes], Fabry disease); inflammatory vasculitides (type 4) (eg, primary angiitis of the central nervous system [PACNS], Susac syndrome, connective tissue disorders such as systemic lupus erythematosus [SLE] and Sjögren syndrome); venous collagenosis (type 5); and other (type 6) (eg, radiation therapy).

Normal White Matter

The central nervous system is composed of neurons and glial cells. Myelinated axons together with glial cells are the main components of the normal white matter. The myelin sheath is produced by oligodendrocytes and is the component responsible for the color and the imaging characteristics of normal white matter. Myelin has a water content of about 40%, and the dry part (60%) is mainly composed of lipids (70%–85%), with a smaller component of proteins (15%–30%). Spinal cord myelin has an even higher lipid-to-protein ratio than the brain. The major lipid components of myelin are cerebrosides and lecithin, and the main protein elements of myelin are proteolipid protein and myelin basic protein, which are more specific to the central nervous system and may serve as antigenic targets in autoimmune processes. For the same reason, another important protein component is myelin oligodendrocyte glycoprotein, which is involved in the formation and maintenance of myelin sheaths and is located in the outermost layer of myelin, serving as a potential target for autoimmunity (2,3).

Autoimmune White Matter Diseases

The autoimmune entities can be multiphasic—the classic prototype is MS and related diseases: tumefactive demyelinating lesions (TDLs), Balo concentric sclerosis, Marburg and Schilder variants, and neuromyelitis optica (NMO). Other autoimmune entities are monophasic, like acute disseminated encephalomyelitis (ADEM) and its more aggressive variant, acute hemorrhagic leukoencephalitis or leukoencephalopathy (Hurst disease).

Multiple Sclerosis

MS is a primary demyelinating disease of unknown etiology (autoimmune category), characterized by perivenular inflammation/demyelination with relative axon preservation, manifesting as periventricular, juxtacortical, infratentorial, and spinal cord lesions at magnetic resonance (MR) imaging. MS is the leading cause of nontraumatic neurologic disability in young adults. Both genetic and environmental factors seem to be involved in the etiology. The prevalence of MS varies widely in different regions of the globe, from 15 to 250 per 100 000. Geographic variability shows MS being more common in regions located further from the equator, such as northern Europe. Women are more frequently affected than men (2:1). Clinical onset is usually between the ages of 20–40 years with a peak at 30 years but can occur at any age. The clinical manifestations are nonspecific, overlapping with those of other inflammatory and noninflammatory entities, and consist of motor, sensory, and autonomic dysfunction. More than half of patients are no longer full ambulatory after 20 years of disease, and overall life expectancy is reduced by 7–14 years (4,5).

The MS spectrum includes radiologically isolated syndrome, clinically isolated syndrome, and clinically definite MS. Clinically definite MS can have a relapsing-remitting course (most frequent); other clinical phenotypes include secondary progressive, primary progressive, or progressive relapsing (least common) (6).

The typical yet nonspecific pathology of MS shows plaques—regions of loss of the normal white matter myelination, usually with preservation of the axons. Classic MS lesions are well-defined, elongated, or oblate, following a perivenular distribution. Plaques are associated with macrophage infiltration, lymphocyte perivascular cuffing, fibrin accumulation, and reactive microglia (Fig 1). High iron deposits in the central nervous system have been found in MS and have been associated with disease activity. While iron deposits in the gray matter were rather diffuse, in the white matter they were usually identified at sites of perivenous inflammation (7).

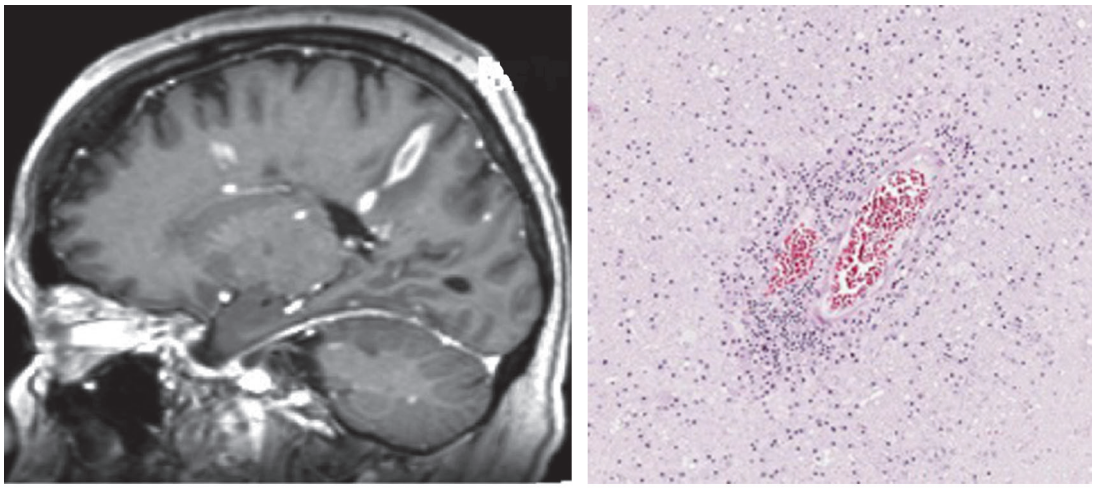

a. b.

Figure 1. MS in a 37-year-old woman. **(a)** Sagittal postcontrast T1-weighted MR image shows typical Dawson fingers: periventricular lesions perpendicular to the ependymal surface with a perivenular distribution. **(b)** Photomicrograph shows perivenular lymphocytic infiltration and demyelination. (Hematoxylin-eosin stain; original magnification, ×200.)

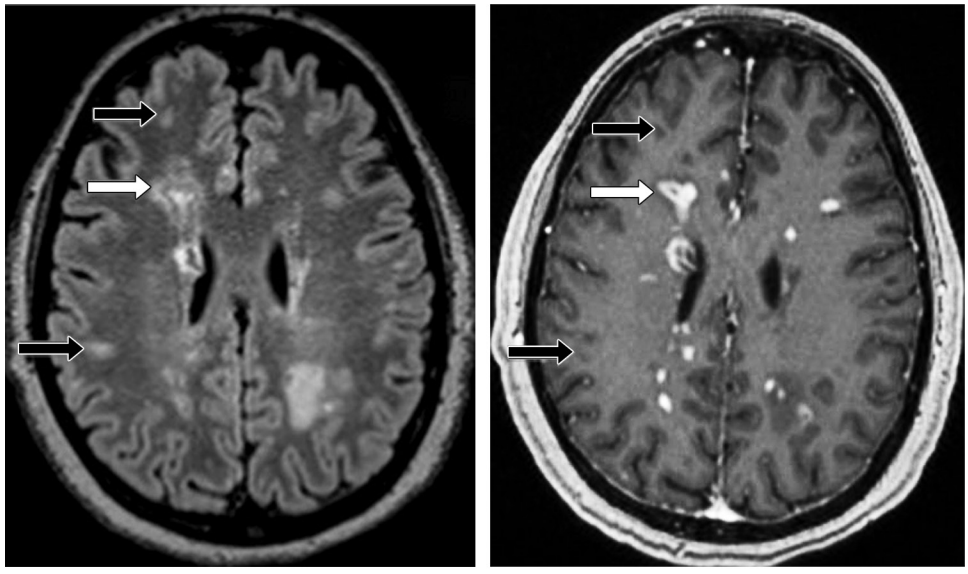

a. b.

Figure 2. MS diagnostic criteria in a single MR imaging examination. **(a)** Axial T2-weighted fluid-attenuated inversion-recovery (FLAIR) image shows periventricular (white arrow) and juxtacortical (black arrows) WMHs, consistent with dissemination in space. **(b)** Axial contrast-enhanced T1-weighted image shows enhancing (white arrow) and nonenhancing (black arrows) lesions, consistent with dissemination in time.

MR imaging is the most important paraclinical tool for diagnosing and monitoring MS (8). The 2010 revised McDonald criteria refer to the geographic and chronologic distribution of MS: dissemination in space requires at least one white matter hyperintensity (WMH) in at least two typical locations such as periventricular, juxtacortical, infratentorial, and spinal cord; dissemination in time requires both contrast-enhancing and nonenhancing lesions in a single MR imaging examination or development of new lesions at follow-up MR imaging (Fig 2) (9,10). New T2 hyperintense and contrast-enhancing WMHs were related to inflammatory activity; the contrast enhancement could last for a variable period, the average being around 3 weeks (11).

Periventricular WMHs in MS are usually ovoid and perpendicular to the ventricle, with perivenular topography—these are the classic Dawson fingers. They abut the ependymal surface, which potentially allows differentiation from nonspecific WMHs and small-vessel disease. MS lesions can also be located around the temporal horn of the lateral ventricle, a region usually spared by small-vessel disease. Using a T2* sequence, a central vein was identified in 45% of MS lesions at 3 T

Table 1: Corpus Callosum Involvement: Differentiating Features of More Common Causes

Disease*	Location	Imaging Characteristics
MS	More frequently the genu and body of the callosum Origin at callososeptal interface	Small separate lesions ("dot-dash") initially Enhancing in acute phase
NMO	More frequently the splenium Entire thickness	Larger, overlapping ("marbled") Enhancing in acute phase
ADEM	Origin at periventricular white matter when present, not from callososeptal interface	Larger Enhancing in acute phase; all the lesions may enhance at the same time (monophasic)
CADASIL	Entire thickness or central	Usually not enhancing
PML	More frequently the genu and splenium	Usually not enhancing
Susac syndrome	Entire thickness or central	Enhancing in acute-subacute phase; inflammation and microinfarcts
Marchiafava-Bignami disease	Middle layers of genu and splenium	Diffusion restriction in acute phase, atrophy in chronic phase
Glioma	More frequently the genu and splenium	Enlarged, heterogeneous enhancement, necrosis
Lymphoma	More frequently the genu and splenium	Enlarged, homogeneous enhancement (unless immunocompromised)
Traumatic/diffuse axonal injury	Splenium > genu, grade II disease	Blooming on T2*-weighted images Diffusion restriction in acute phase

*CADASIL = cerebral autosomal-dominant arteriopathy with subcortical infarcts and leukoencephalopathy, PML = progressive multifocal leukoencephalopathy.

and 87% of MS lesions at 7 T, versus only 8% of nonspecific WMHs at 7 T in healthy volunteers (12). Lesions that are dark on T1-weighted images ("black holes") correlate with severe histologic damage, higher degree of demyelination, and axonal loss (13). Owing to iron accumulation in MS, intralesional susceptibility signal may be observed on T2* images (8,14).

Corpus callosum lesions in early MS are characteristically found at the callososeptal interface, are usually focal and discrete producing the subcallosal "dot-dash" appearance, and are often easier to visualize on sagittal T2-weighted images. They have been reported more frequently in the genu and body of the callosum (15). The differential diagnosis of corpus callosum involvement (Table 1) (Fig 3) includes other primary or secondary demyelinating processes (NMO, ADEM, CADASIL, Susac syndrome, PML, Marchiafava-Bignami disease), neoplasms (lymphoma, glioma, gliomatosis cerebri—the latter may mimic white matter disease only by its extension), and traumatic injury (traumatic/diffuse axonal injury).

Isolated juxtacortical WMHs in MS involve the subcortical U-fibers and are another classic location. Cortical lesions, on the other hand, have become increasingly recognized in MS and are expected to have more prognostic and diagnostic value in the future. They occur early, have been found in clinically isolated syndrome, and have been associated with cognitive impairment. Cortical lesions are small and more conspicuous on double inversion-recovery images and at high magnetic field strengths (16–18).

The McDonald diagnostic criteria also include infratentorial location. Brainstem lesions in MS are characteristically peripheral (as opposed to central in small-vessel disease), are commonly asymmetric or unilateral, and are usually well-defined (19). Cerebellar lesions usually affect the larger white matter structures—like the brachium pontis (middle cerebellar peduncle)—although the smaller cerebellar peduncles and hemispheric white matter may also be affected.

Spinal cord lesions are reported in 30%–40% of cases of clinically isolated syndrome and up to 90% of cases of clinically definite MS (13). The cervical cord is most frequently involved and sometimes is the cause of death (Fig 4). Typically, the lesions are well-defined, less than one to two vertebral segments in craniocaudal dimension, and less than 50% of the cross-sectional area of the spinal cord in the axial plane, often affecting the peripheral white matter. Extensive spinal cord swelling is uncommon. Active lesions may enhance, albeit less frequently than brain lesions. Occasionally cord atrophy is seen, especially in upper segments, in long-standing and progressive MS (20). The homologue of MS regarding the chronic multiphasic

Figure 3. Differential diagnosis of corpus callosum lesions. **(a)** Susac syndrome: sagittal postcontrast T1-weighted image shows a large "snowball" lesion that involves the entire thickness of the body of the corpus callosum. **(b)** CADASIL: sagittal T1-weighted image shows multiple lesions in the corpus callosum; note the involvement of the entire callosal thickness and the low T1 signal intensity ("black holes"). (Courtesy of John H. Rees, MD, Partners Imaging Center, Sarasota, Fla.) **(c)** Marchiafava-Bignami disease: axial diffusion-weighted image shows restricted diffusion in the splenium of the corpus callosum. **(d)** PML: axial T2-weighted FLAIR image shows a confluent right occipital subcortical white matter lesion, with extension across the splenium of the corpus callosum. (Courtesy of Jacqueline A. Bello, MD, Montefiore Medical Center, Bronx, NY.)

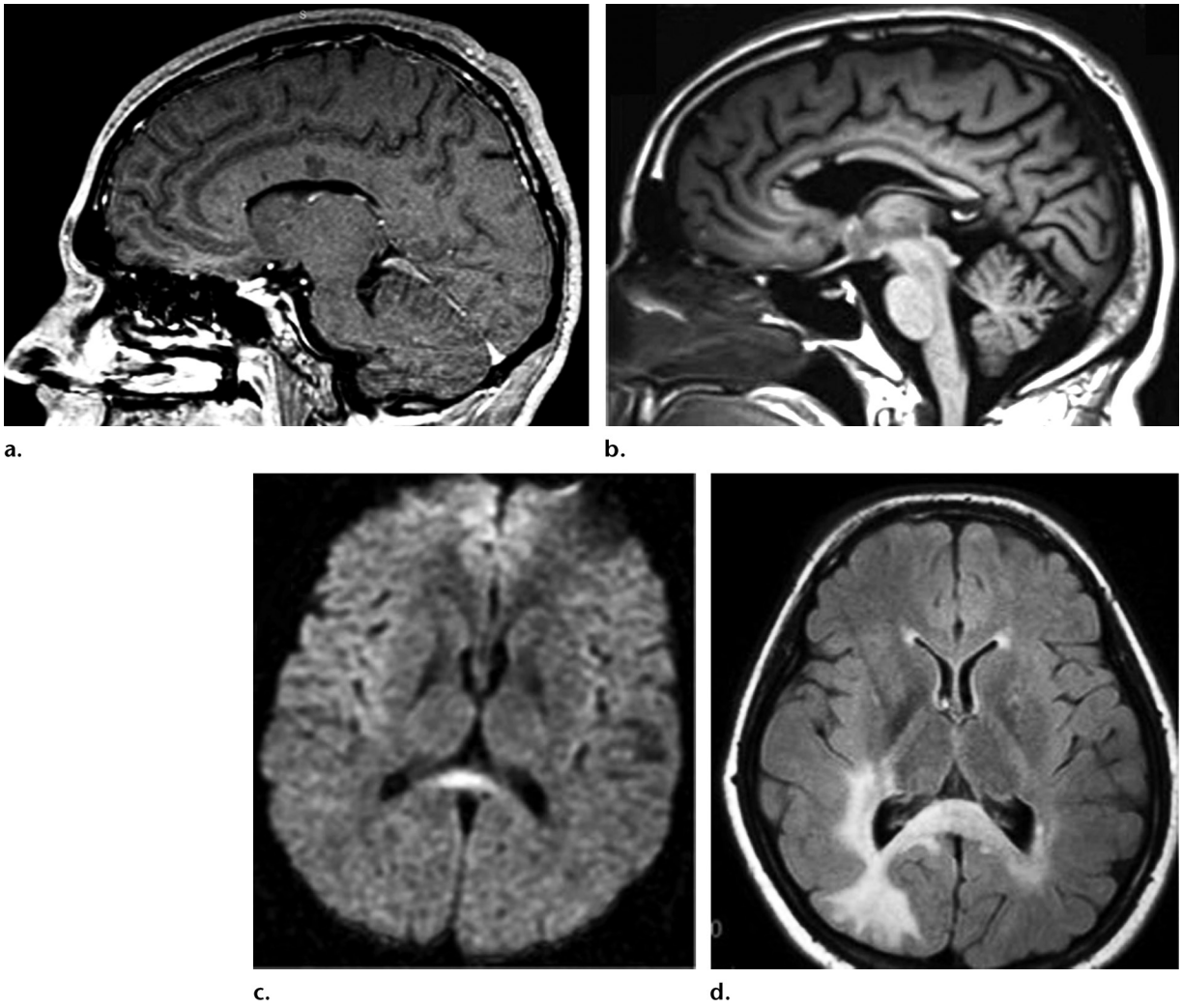

Figure 4. MS. Autopsy specimen shows extensive demyelination (lighter regions) involving the medulla oblongata. (Luxol fast blue stain.)

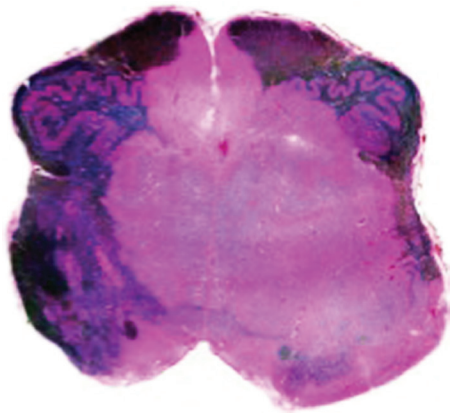

course, but involving the peripheral nervous system, is chronic inflammatory demyelinating polyradiculoneuropathy.

Optic neuritis is usually a clinical diagnosis, and the necessity for MR imaging depends on the clinical context. If the diagnosis of MS is already established, imaging of the optic nerve is not required unless atypical symptoms are present, when MR imaging may be performed to rule out alternative diagnoses. On the other hand, when optic neuritis is the first presentation, the role of MR imaging is mainly to assess the brain for additional lesions.

Overall, diagnosis of MS is based on the clinical history, cerebrospinal fluid analysis (oligoclonal bands, immunoglobulin G), visual evoked

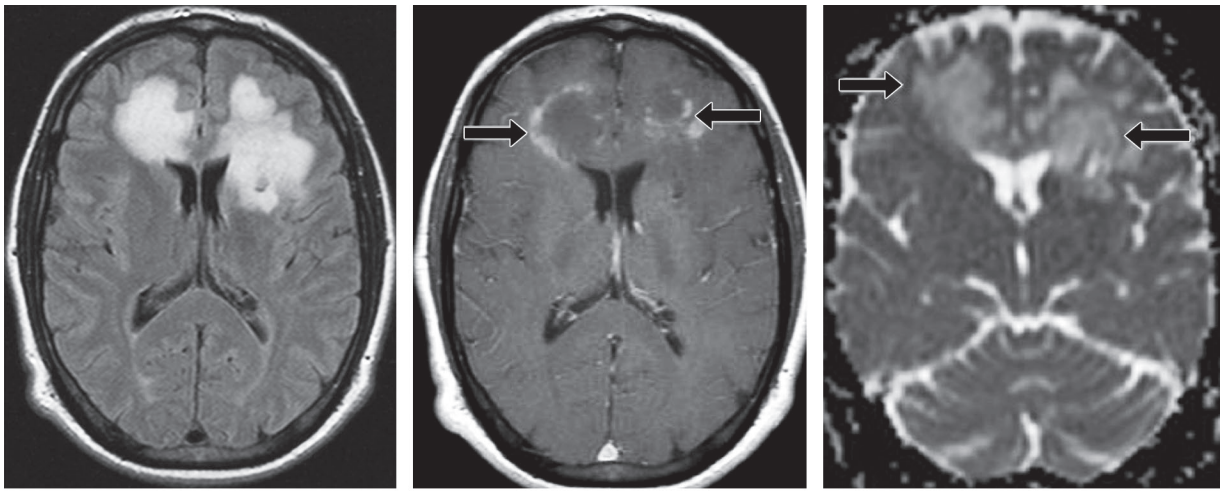

a. b. c.

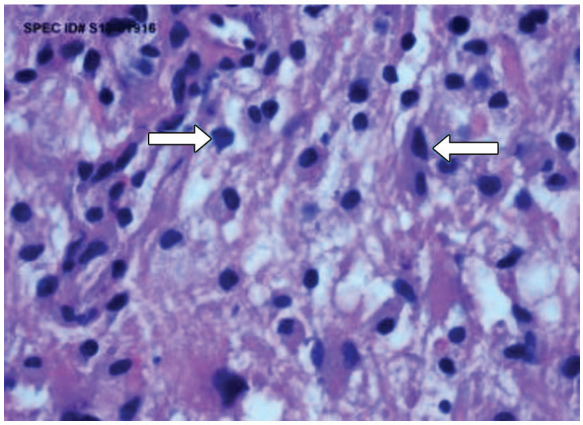

d.

Figure 5. TDLs in a 49-year-old man. **(a)** Axial T2-weighted FLAIR image shows bilateral confluent hyperintense areas in the subcortical and periventricular white matter, which extend toward the genu of the corpus callosum and abut the ependymal surface. **(b)** Axial postcontrast T1-weighted image shows incomplete or open ring enhancement (arrows), consistent with the advancing front of demyelination. Note the lack of any significant perilesional edema or mass effect, given the size of the lesion. **(c)** Axial apparent diffusion coefficient (ADC) map shows a peripheral rim of subtle restricted diffusion (arrows), likely related to inflammatory hypercellularity. **(d)** Photomicrograph shows scattered foamy/vacuolated macrophages (arrows). (Hematoxylin-eosin stain; original magnification, ×200.)

potential abnormalities, MR imaging, and "no better explanation." Nevertheless, misdiagnosis of MS is frequent, mainly due to MR imaging pitfalls, leading to use of MS-modifying therapy in about one-fourth of these patients otherwise without MS. Top causes in patients misdiagnosed with MS based on brain MR imaging findings are nonspecific WMH, ischemic small-vessel disease, migraine, NMO, CADASIL, and ADEM (21).

Relatives or Variants of MS

Tumefactive Demyelinating Lesions.—TDLs are defined as large demyelinating lesions (>2 cm) and can be solitary or few in number. Difficulty in making the correct diagnosis may lead to biopsy, and the extensive presence of macrophages and myelin loss could suggest a demyelinating process. Nevertheless, the pathologic findings at biopsy are nonspecific and could be confusing because of hypercellularity, atypical reactive astrocytes, and mitotic figures, which are also observed in glial neoplasms.

Thus, TDLs can be mistaken for high-grade enhancing neoplasms—possible clues to the diagnosis include an incomplete ring of enhancement and/or restricted diffusion reflecting the advancing front of demyelination, a paucity of perilesional edema, relative lack of mass effect for lesion size, and lower cerebral blood volume at perfusion imaging (Fig 5). Also, TDLs are inflammatory processes and may have a higher quantity of water than many tumors, which translates into lower attenuation at computed tomography (CT) and higher signal intensity on T2-weighted images. They do not always produce proportional mass effect—"nontumefactive" TDL—thus, the term *tumefactive* can be a misnomer. MR spectroscopy could show elevated choline or lactate peaks with higher inflammatory activity, but this is nonspecific and can also be seen in neoplasms. Follow-up MR imaging, especially after immunosuppressive treatment, frequently demonstrates diminution of the lesions (22–24).

Marburg Variant.—This rare variant represents the classic fulminant form of idiopathic inflammatory demyelination and usually occurs in young adults (aka acute fulminant MS). Pathologically, it is characterized by massive macrophage infiltration with severe inflammation, necrosis, and extensive destruction. Classic MR imaging findings are multifocal WMHs with confluence into larger areas and extensive dissemination. Death usually occurs

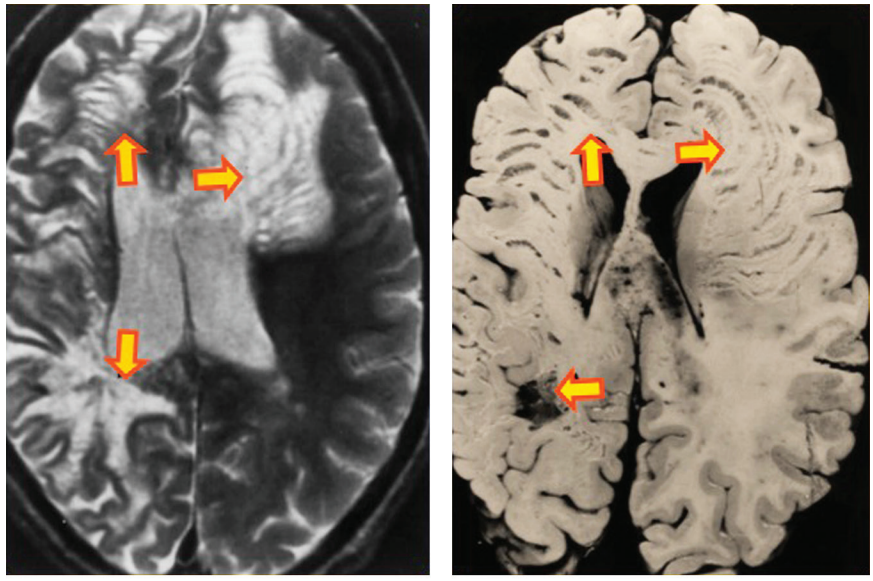

Figure 6. Balo concentric sclerosis in a 32-year-old woman. **(a)** Axial T2-weighted image shows extensive hyperintense lamellated white matter lesions in both cerebral hemispheres (arrows), with involvement of the subcortical U-fibers, and mild mass effect in the left frontal region. **(b)** Gross specimen shows bandlike areas of demyelination alternating with normal myelination (arrows). **(c)** Photomicrograph shows concentric bands of demyelination and remyelination. (Luxol fast blue stain; original magnification, ×200.)

a. **b.**

c.

from brainstem involvement. To some degree, it resembles severe forms of ADEM (23).

Balo Concentric Sclerosis.—This rare and severe acute monophasic process is characterized by concentric rims of myelin destruction and repair, frequently involving the centrum semiovale and corona radiata. These alternating layers of demyelinated, remyelinated, and normal myelinated white matter give the typical appearance of hyperintense-isointense-hypointense concentric rings on T2-weighted images ("onion bulb") (Fig 6). Peripheral restricted diffusion and contrast enhancement are common and represent the advancing front of demyelination (23).

Schilder Disease.—Schilder disease (diffuse myelinoclastic sclerosis) is a rare variant that usually affects children and is characterized by acute or subacute evolution, which may respond to corticosteroids. Pathologic, radiologic, and clinical features are somewhat similar to those of TDL, raising the hypothesis that it just might be a childhood form of TDL. Unlike Marburg disease, it usually spares the brainstem (23).

Neuromyelitis Optica

NMO (Devic disease) is a demyelinating disease of autoimmune etiology induced by NMO–immunoglobulin G, an autoantibody against aquaporin-4 water channels. The aquaporin-4 channel is found in astrocytes, belongs to the family of integral membrane proteins that conduct water through the cell membrane, and has higher expression along the pathway between the third and fourth ventricles. The antibodies seem to target the regions where the blood-brain barrier is weaker and the expression of aquaporin-4 is higher. The spinal cord and optic nerve are preferential targets, probably because of the increased permeability of the blood-brain barrier at these levels. The underlying pathogenesis has not been completely elucidated; the disease is mainly sporadic, and some viruses share immunogenic features of aquaporin-4.

The prevalence ranges from 0.5 to 4.4 per 100 000, being more common in Asian, Indian, and African populations. The age of onset varies widely, with an average age of 41 years in the United States. Women are more commonly affected, with a ratio of 6.5:1. Up to 90% of cases have a recurrent course with more dramatic relapses than MS. If misdiagnosed and treated as ordinary MS, a further exacerbation can be produced. The classic triad of NMO consists of myelitis, optic neuritis, and positive NMO–immunoglobulin G. The optic neuritis can be unilateral or bilateral (Fig 7). NMO–immunoglobulin G has more than 90% specificity and 70%–90% sensitivity for the disease (25–28). Myelitis and optic neuritis may occur synchronously

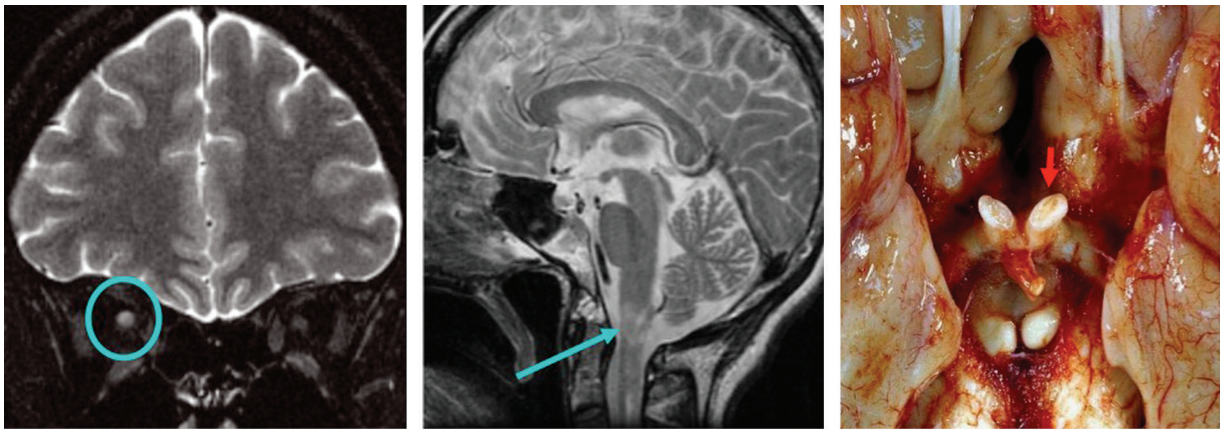

a. b. c.

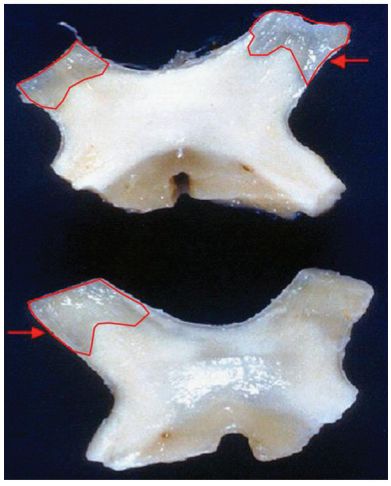

d.

Figure 7. NMO in a 39-year-old woman. **(a)** Coronal T2-weighted image shows hyperintensity and swelling of the right optic nerve due to optic neuritis (circle). **(b)** Sagittal T2-weighted image shows patchy hyperintensity involving the medulla oblongata and cervical cord (arrow), consistent with myelitis. **(c)** Autopsy specimen shows areas of demyelination in the prechiasmatic portions of the optic nerves (arrow). The granular appearance of the optic nerves suggests demyelination from NMO. **(d)** Magnified cross-section views through the chiasm show a more gelatinous demyelination (arrows), which may also occur in MS. (Fig 7c and 7d courtesy of Robert E. Schmidt, MD, PhD, Washington University, St Louis, Mo.)

or metachronously, and episodes of one without the other occur in many patients.

Unlike MS, myelitis in NMO is longitudinally and transversally extensive, often involving three or more vertebral segments, and is more frequently inhomogeneous. "Bright spotty lesions," a newly described spinal finding in NMO, refers to this heterogeneous appearance on axial T2-weighted images and can help differentiate NMO from MS (29).

Brainstem lesions in NMO are typically dorsal (up to 90%) and in the periaqueductal regions due to the higher concentration of aquaporin-4. NMO has a higher frequency of medulla oblongata lesions but lower frequency of pons lesions compared with MS and ADEM. NMO lesions typically have poorly defined margins (90%). Brainstem lesions in NMO are usually asymmetric or unilateral (up to 90%) (19).

NMO was named for selective involvement of the spinal cord and optic nerves, with relative sparing of the brain, in contrast to MS. This is generally valid for early stages, when brain lesions are either absent or few and nonspecific. However, usually later, brain lesions do occur, with a predilection for periependymal regions, the hypothalamus, and the pathway between the third and fourth ventricles. Longitudinal corticospinal tract lesions have also been reported. Recent studies have described tiny WMHs in the subcortical white matter, usually not traversed by a central venule at high magnetic field imaging (30). Furthermore, advanced MR imaging techniques such as diffusion tensor imaging have demonstrated abnormalities in otherwise normal-appearing white and gray matter. Cortical and basal nuclei lesions were uncommon, and brain lesions were more commonly reported in Asians (25,26).

Corpus callosum lesions in NMO preferentially involve the splenium. Compared with those in MS, they are larger, more confluent, more edematous, and more heterogeneous. The "marbled pattern" represents multiple overlapping heterogeneous lesions in the corpus callosum and has been described in the acute phase of NMO (31).

Acute Disseminated Encephalomyelitis

ADEM is also mediated by antigen-antibody complexes and usually occurs in children (typically <15 years old), often within 2 weeks after an antigenic challenge—either an infection (50%–75%, frequently upper respiratory) or a vaccination. The incidence of ADEM has been reported to be 0.4 per 100 000 person-years. ADEM partially overlaps with other demyelinating diseases, although there are some differentiating features (Fig 8). In contrast to the female predilection of MS and NMO, ADEM has little

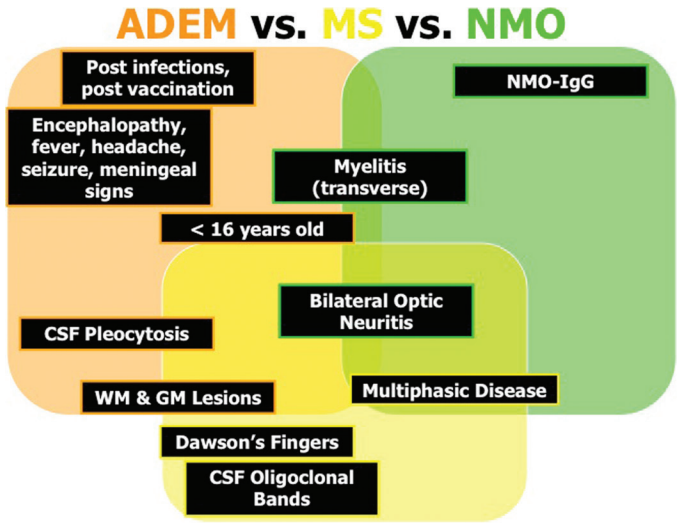

Figure 8. Differential diagnosis of ADEM, MS, and NMO. *CSF* = cerebrospinal fluid, *GM* = gray matter, *IgG* = immunoglobulin G, *WM* = white matter.

to no gender predilection (slightly more frequent in males) (32). Common clinical manifestations are encephalopathy, fever, headache, seizure, multiple focal deficits, and meningeal signs.

The course is monophasic in 90% of cases, but there is the possibility of relapses within the first 3 months. Anti-MOG (myelin oligodendrocyte glycoprotein) immunoglobulin G antibodies are present in one-half of patients with ADEM, and cerebrospinal fluid pleocytosis is frequently present. The outcome of ADEM is variable; most patients experience complete recovery, with notable improvement or complete remission at follow-up MR imaging, although mortality in the initial phase can be as high as 10%–20% (23,27,33). It is also believed that a subset of patients will later progress to MS, although this could also mean that the first presentation of MS was initially misdiagnosed as ADEM.

Although initially considered not to be a perivenular process like MS, recent pathologic advances have revealed a diffuse perivenular inflammation as the underlying process leading to confluent areas of demyelination (19,23).

The lesions in ADEM are multiple and bilateral and can involve both brain and spine, both white matter and gray matter. Compared with MS lesions, ADEM lesions can be more rounded and larger with poorly defined margins and more prominent involvement of the deep gray matter nuclei, thalamus, and brainstem (Fig 9). Subcortical WMHs and U-fiber involvement are frequently observed. Corpus callosum involvement in ADEM can sometimes be seen; the lesions are larger than in MS and do not usually arise from the callososeptal interface.

As a reflection of the monophasic course of ADEM, MR imaging should not reveal signs of previous white matter demyelination and the lesions may enhance at the same time, unless relapses occur in the first 3 months. As in the other inflammatory processes, the advancing front of demyelination can appear as a peripheral rim of contrast enhancement or restricted diffusion. In more severe cases of ADEM, petechial hemorrhages can be seen (Fig 10). As in TDL, elevated choline and lactate levels can be observed at MR spectroscopy in lesions with higher inflammatory activity. Brainstem lesions in ADEM more frequently involve the ventral midbrain and are usually bilateral and symmetric with poorly defined margins (19).

Myelitis, included in the names of both NMO and ADEM, is virtually always present and is a

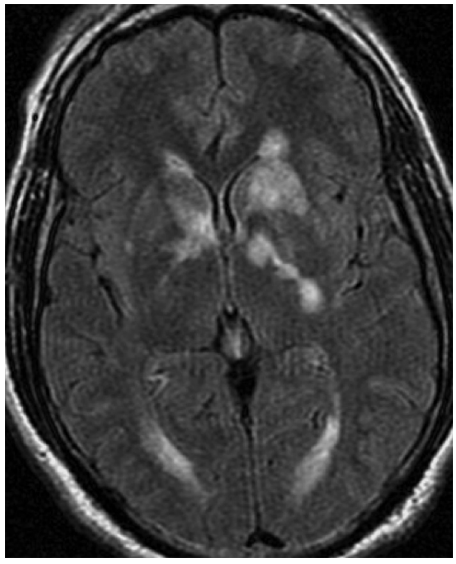

Figure 9. ADEM in a 12-year-old girl. Axial T2-weighted FLAIR image shows bilateral hyperintense lesions involving the deep gray matter nuclei and periventricular-subcortical white matter. (Courtesy of Steven J. Goldstein, MD, Lexington, Ky.)

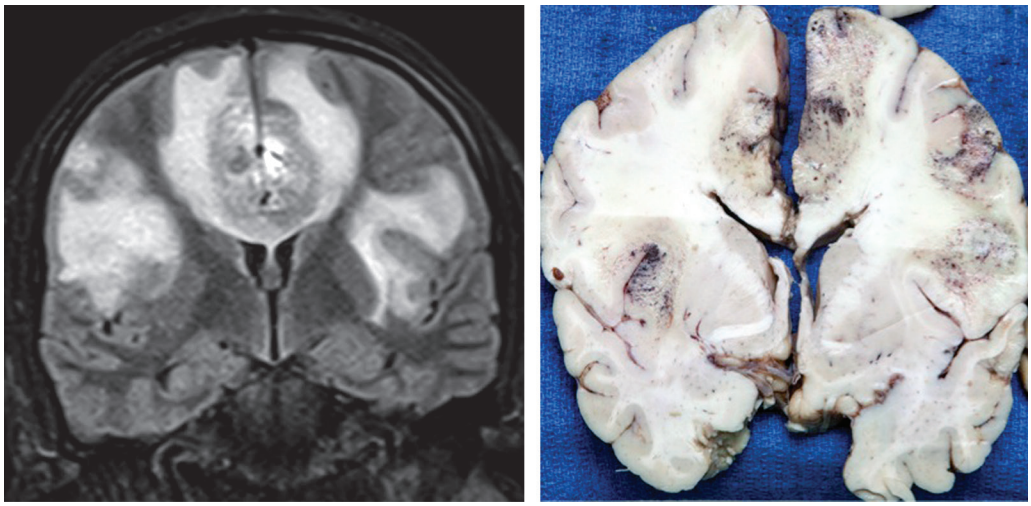

a. b.

Figure 10. ADEM in a 28-year-old woman. Coronal T2-weighted FLAIR image **(a)** and correlative gross specimen **(b)** at a similar level show extensive periventricular and subcortical white matter involvement. Note the multiple scattered foci of microhemorrhage at the corticosubcortical interface, visible only at pathologic analysis.

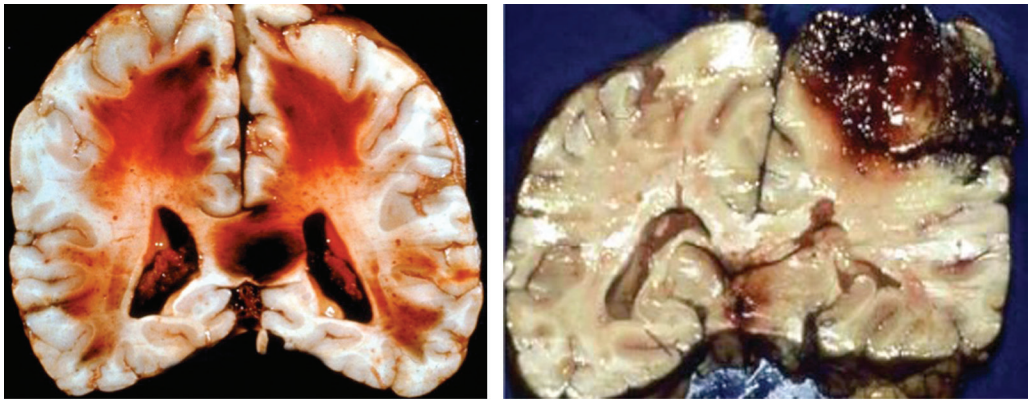

a. b.

Figure 11. AHL manifesting as the diffuse form **(a)**, with extensive bilateral hemorrhagic areas involving the cerebral white matter, or the pseudotumoral form **(b)**, with localized hemorrhage and necrosis.

criterion for diagnosing NMO, yet is seen in only up to one-third of patients with ADEM. Spinal cord lesions in ADEM can have a confluent appearance with swelling or a pattern similar to that of transverse myelitis. The homologue of ADEM regarding the acute monophasic course, but involving the peripheral nervous system, is acute inflammatory demyelinating polyneuropathy (AIDP or Guillain-Barré syndrome).

Longitudinal MR imaging could be used to support the diagnosis, usually showing notable improvement or remission in ADEM, while frequently new lesions will occur over time in MS and NMO.

Acute Hemorrhagic Leukoencephalitis

AHL (Hurst disease) is a rare and more aggressive form of ADEM, typically with fulminant evolution to death in a few days to weeks. As in ADEM, a previous upper respiratory tract infection is common. Pathologically, extensive inflammation, necrosis, and petechial hemorrhages are observed. Imaging features of AHL are similar to those of ADEM but typically larger in extent, with more mass effect, brain swelling, and foci of restricted diffusion. Hemorrhages, better depicted on T2*-weighted images, are key findings due to autoimmune vascular injury in AHL. While hemorrhages can also be seen in severe cases of ADEM, they should always be present in AHL, if not at imaging then at autopsy in either diffuse or localized/pseudotumoral forms (Fig 11) (23).

Infectious White Matter Diseases

The infectious leukoencephalopathies can be multifocal (eg, Lyme disease) or may be confluent in appearance (eg, PML and human immunodeficiency virus [HIV] encephalopathy).

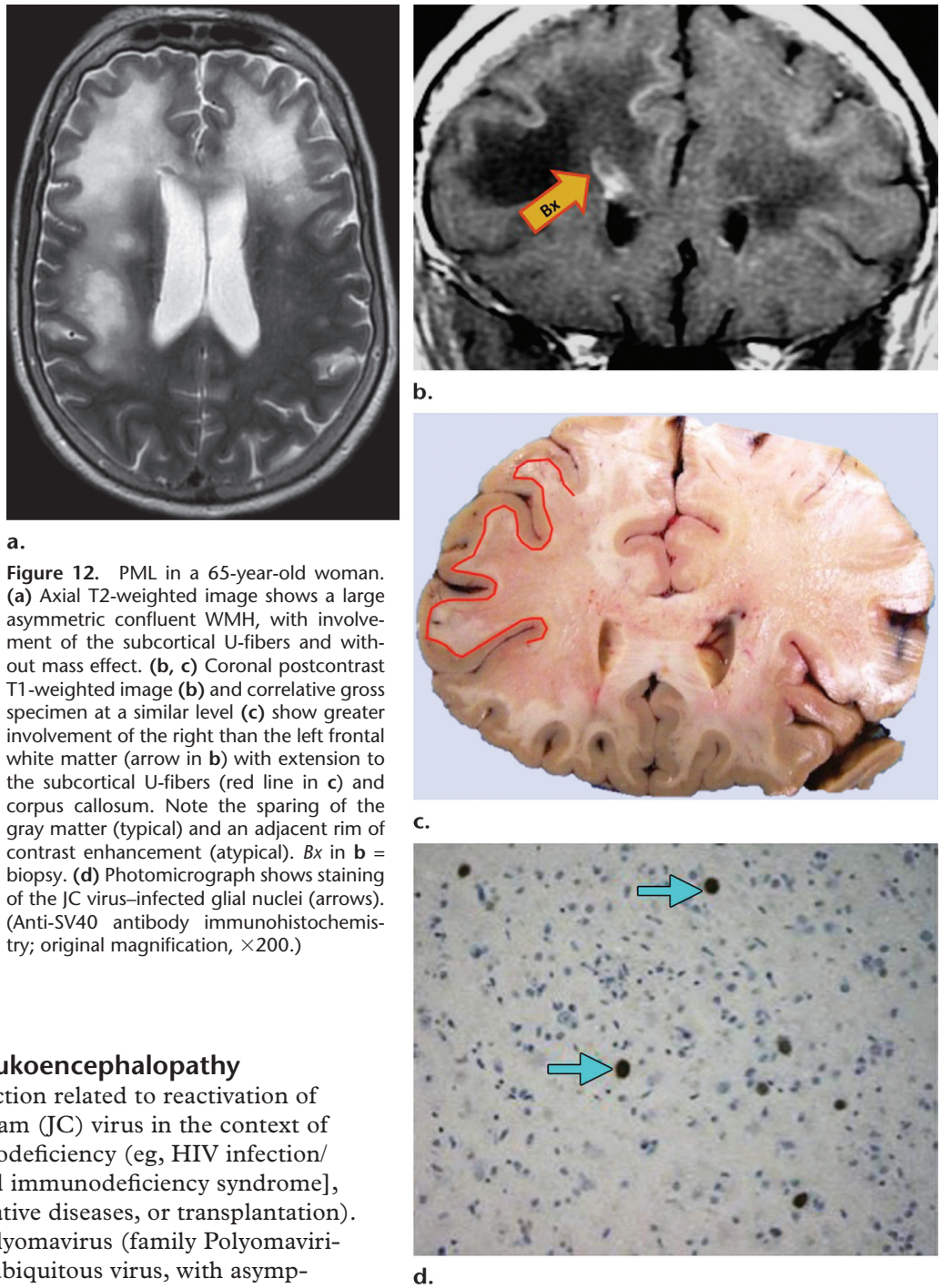

a.

b.

c.

d.

Figure 12. PML in a 65-year-old woman. **(a)** Axial T2-weighted image shows a large asymmetric confluent WMH, with involvement of the subcortical U-fibers and without mass effect. **(b, c)** Coronal postcontrast T1-weighted image **(b)** and correlative gross specimen at a similar level **(c)** show greater involvement of the right than the left frontal white matter (arrow in **b**) with extension to the subcortical U-fibers (red line in **c**) and corpus callosum. Note the sparing of the gray matter (typical) and an adjacent rim of contrast enhancement (atypical). *Bx* in **b** = biopsy. **(d)** Photomicrograph shows staining of the JC virus–infected glial nuclei (arrows). (Anti-SV40 antibody immunohistochemistry; original magnification, ×200.)

Progressive Multifocal Leukoencephalopathy

PML is an infection related to reactivation of John Cunningham (JC) virus in the context of cellular immunodeficiency (eg, HIV infection/AIDS [acquired immunodeficiency syndrome], lymphoproliferative diseases, or transplantation). JC virus is a polyomavirus (family Polyomaviridae). This is a ubiquitous virus, with asymptomatic infection in the normal population and latent persistence in the kidney and cerebrum. Patients with a CD4 cell count below 100 are at higher risk for reactivation of the JC virus. PML has been found in 5% of autopsies in AIDS. The diagnosis is supported by the presence of JC antigen in cerebrospinal fluid. Survival was historically poor at 2–6 months but has improved with antiretroviral therapy, now up to 3–4 years.

In patients with PML, JC virus is present in circulating B lymphocytes and is responsible for infection and lysis of oligodendrocytes, which leads to failure in producing myelin and large geographic areas of demyelination. Radiologically, there are confluent asymmetric lesions with a predilection for peripheral white matter and subcortical U-fibers. Typically, there is relatively little mass effect, given the size of the lesion (Fig 12). Classically, there is no significant contrast enhancement, although it can be seen in subsequent immune reconstitution inflammatory syndrome (IRIS) after initiation of antiretroviral therapy for AIDS, in PML related to MS-specific therapy (eg, natalizumab), and has been linked to improved survival. PML may also involve the corpus callosum (34).

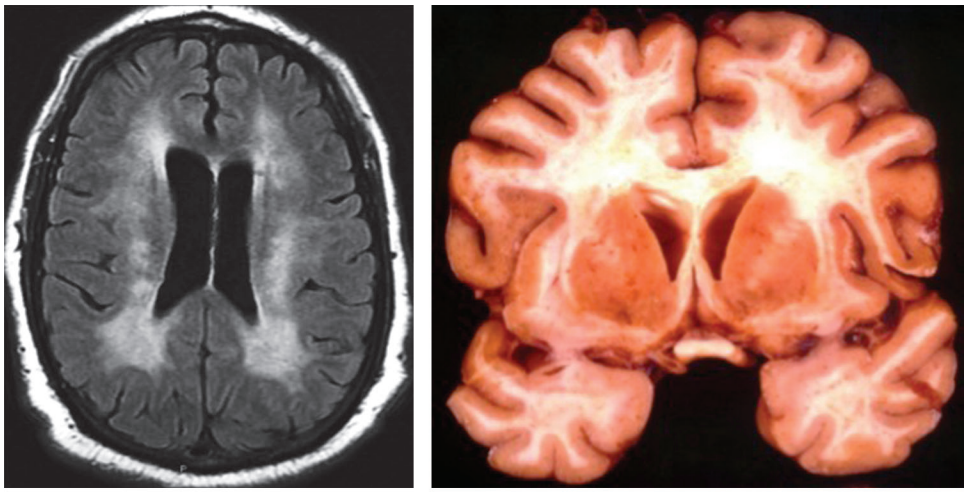

a. b.

Figure 13. HIV encephalopathy in a 27-year-old man. **(a)** Axial T2-weighted FLAIR image shows symmetric periventricular white matter involvement with some prominence of ventricles for the age of the patient. **(b)** Gross specimen shows diminution of global brain volume.

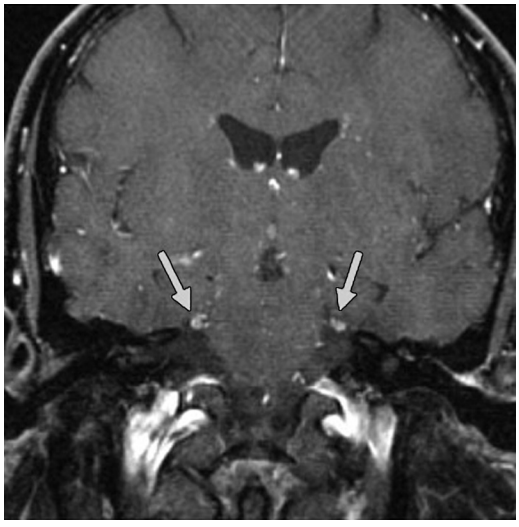

Figure 14. Lyme disease in a 21-year-old man. Coronal postcontrast T1-weighted image shows enhancement of the trigeminal nerves (arrows). Abnormal leptomeningeal enhancement may serve as a distinguishing feature from MS (WMHs can be seen in both diseases).

HIV Encephalopathy

HIV encephalopathy is also known as AIDS dementia complex (ADC). It is a consequence of direct infection of microglia by HIV. Despite improved survival as a consequence of effective antiretroviral therapies, HIV encephalopathy occurs in 15%–20% of AIDS patients and is a major cause of morbidity. Patients with a lower CD4 cell count, longer disease duration, and older age are at higher risk. Indirect effects of infected macrophages include the release of neurotoxic agents (quinolinic acid).

Pathologically, diffuse and marked periventricular demyelination, neuronal loss, astroglial proliferation, and vacuolar changes are observed. Imaging studies show diffuse bilateral and symmetric periventricular WMH, preferentially affecting the more central white matter without mass effect or enhancement. Brain atrophy is a hallmark of the disease (Fig 13). HIV encephalopathy shares some features with PML: both cause confluent white matter lesions without significant mass effect or enhancement, but more peripheral and asymmetric in PML (infecting oligodendrocytes) versus more central and symmetric in HIV encephalopathy (infecting microglia) (34).

Lyme Disease

Borreliosis (Lyme disease) is a zoonosis transmitted by tick bite (*Ixodes* species) and is the most common vector-transmitted disease in the United States, with an incidence of 9.7 per 100 000 person-years. It is usually caused by the spirochete *Borrelia burgdorferi* in the United States and *B garinii* or *B afzelii* in Europe. Initial manifestations include erythema migrans (targetlike rash) and flulike syndrome. Neurologic and cardiac anomalies can be seen after weeks to months. Central nervous system involvement seems to be the result of an abnormal autoimmune reaction and occurs in 10%–15% of patients with Lyme disease, less common in the United States (<10%) than in Europe (>35%).

Cerebrospinal fluid analysis may show pleocytosis with lymphocyte predominance and elevated protein level. Detection of serum or cerebrospinal fluid antibodies supports the diagnosis. Imaging findings include multifocal WMH with variable enhancement, most commonly in the frontal and parietal regions, sometimes in the basal nuclei and brainstem. Corpus callosum lesions may sometimes occur, mimicking MS. Leptomeningeal and cranial nerve enhancement may also be present, which can help in differentiation from MS (Fig 14) (35).

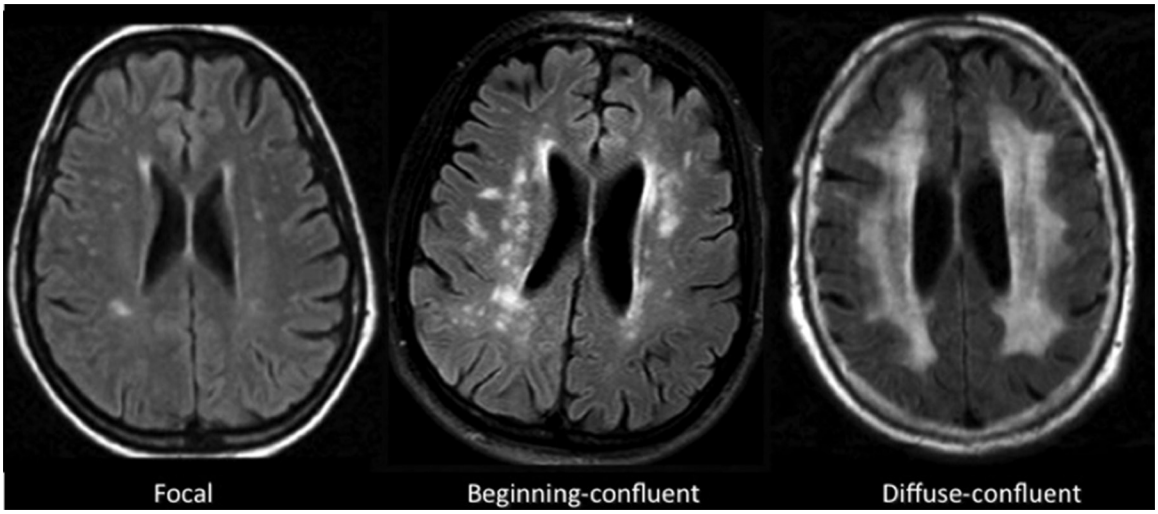

Figure 15. Axial T2-weighted FLAIR images show the WMH rating scale for small-vessel disease.

Vascular White Matter Diseases: Small-Vessel Disease

Small-vessel disease is by far the leading cause of white matter disease and can be divided into six types: arteriolosclerosis (type 1); cerebral amyloid angiopathy (type 2); inherited vasculopathies (type 3) (eg, CADASIL, MELAS [*m*itochondrial myopathy, *e*ncephalopathy, *l*actic *a*cidosis, *s*trokelike episodes], Fabry disease); inflammatory vasculitides (type 4) (eg, primary angiitis of the central nervous system [PACNS], Susac syndrome, connective tissue disorders such as systemic lupus erythematosus [SLE] and Sjögren syndrome); venous collagenosis (type 5); and other (type 6) (eg, radiation therapy) (36).

Small-vessel disease is a common cause of cognitive and physical disability, contributing to up to 45% of dementias—second only to Alzheimer disease. It also accounts for around 20% of strokes (37).

Small-Vessel Disease Related to Arteriolosclerosis

This is an extremely common condition, related to aging and vascular risk factors (eg, hypertension). Pathologic analysis demonstrates fibrohyaline material in the vessel wall with lipohyalinosis, microatheroma, fibrinoid necrosis, thickening of the walls, and narrowing of the lumen. Muscle loss from the media leads to loosening of the wall and microaneurysm formation. Since it is a systemic process, similar findings are seen in other targets for small-vessel disease, such as the retina and kidneys (36).

Despite considerable advances, small-vessel disease mechanisms are incompletely elucidated. Besides diagnosing and reflecting the degree of involvement, imaging could give important insights into the pathologic substrate. A problem that hampers progress is the wide heterogeneity of the radiologic language (37). In an attempt to overcome this, an international task force drafted a consensus, classifying small-vessel disease as WMHs, recent small subcortical infarcts, lacunes, microbleeds, and brain atrophy (37).

WMHs occur in 80% of whites over the age of 60 years, with a predilection for the frontal and parietal regions (38). The degree of WMH can be rated as focal, beginning confluent, and diffuse confluent (Fig 15) (39,40). WMHs occur in vascular end zones, which at the supratentorial level are located in the basal nuclei, corona radiata, and centrum semiovale (41). In the brainstem, they appear centrally due to the centripetal pattern of feeding vasculature, with the vascular end zone in the deeper brainstem (42). WMHs are considered the "tip of the iceberg," reflecting an underlying process with no visible boundaries at MR imaging. WMHs have been correlated with cognitive, behavioral, gait, and urinary impairment and have been shown to progress over time (36,43,44).

Recent small subcortical infarcts or acute lacunar infarcts are defined as infarcts less than 20 mm; they can progress to lacunes or WMHs without cavitation or may disappear (45). Lacunes are defined as round/ovoid cavities of 3–15 mm that follow the signal intensity of cerebrospinal fluid (37). Recent small subcortical infarcts occur in the territory of perforating arterioles and may evolve into lacunes in the chronic phase; these small fluid-filled lesions often appear next to WMHs, reflecting an interrelated pathogenic substrate for both lacunes and WMHs (ie, small-vessel disease of perforating arterioles) (41). Perivascular spaces (Virchow-Robin) also have the signal intensity of cerebrospinal fluid and follow the course of penetrating vessels, but appear linear when imaged parallel to the vessel and the shortest diameter is often less than 3 mm,

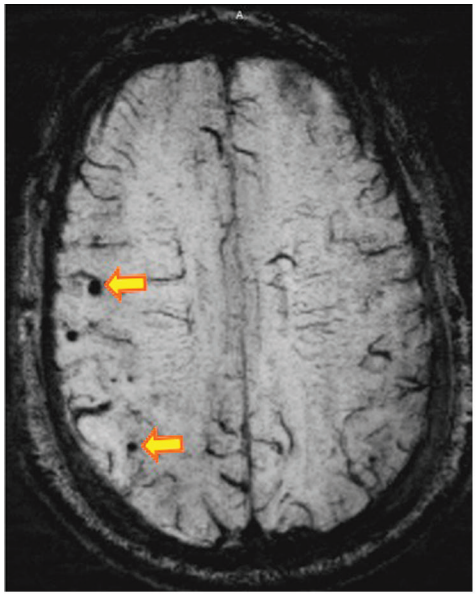

a.

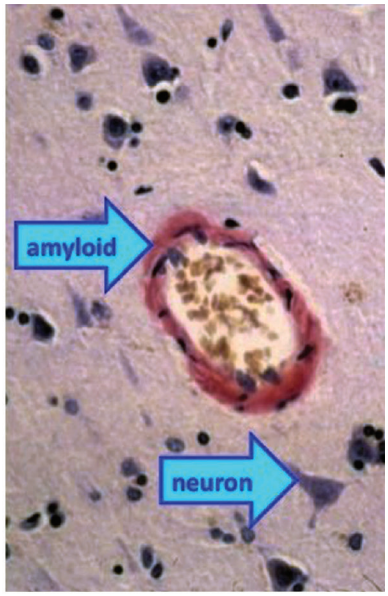

c.

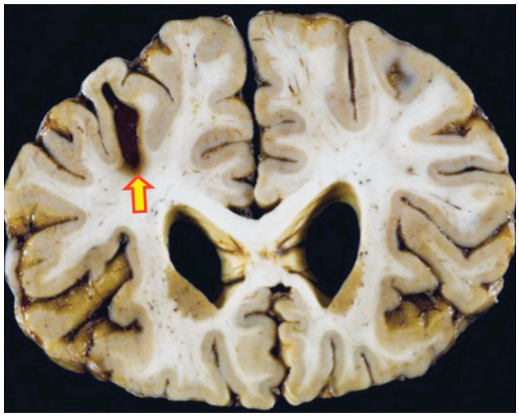

b.

Figure 16. Cerebral amyloid angiopathy in a 77-year-old man. **(a)** Axial susceptibility-weighted image shows microbleeds at the corticosubcortical interface (arrows). **(b)** Gross pathologic specimen shows a peripheral lobar hematoma in the right frontal region (arrow). **(c)** Photomicrograph shows β-amyloid deposits in the vessel wall. (Congo red stain; original magnification, ×200.)

although spaces larger than 1 cm are occasionally observed. Another differentiating feature could be a surrounding rim of hyperintensity on T2-weighted FLAIR images, typically accompanying lacunes but not perivascular spaces. Multiple perivascular spaces involving the basal nuclei are known as "état criblé" and can be seen with atrophy and aging (37,46).

Cerebral microhemorrhages are defined as small (up to 5-mm) areas of signal void/blooming on paramagnetic-sensitive images (T2*-weighted gradient-echo or susceptibility-weighted imaging), while usually not visible with other sequences or at CT. When related to chronic hypertension and arteriolosclerosis, they are typically found in the deep gray matter and must be differentiated from calcifications, normal vessels, iron deposits from other causes, hemorrhagic metastases, and traumatic brain injury (37,47).

Another manifestation of small-vessel disease is brain atrophy, defined as generalized enlargement of cerebrospinal fluid spaces. It is best evaluated on axial T2-weighted FLAIR images, and reading scales are available (48). Tissue loss from large-vessel infarcts, trauma, or other focal lesions is not classified as small-vessel disease–related brain atrophy (37).

Cerebral Amyloid Angiopathy

Cerebral amyloid angiopathy is a vasculopathy caused by β-amyloid deposition in the media and adventitia of cortical and leptomeningeal arteries and seems to involve the occipital and frontal regions more frequently. Systemic amyloidosis is not a predisposing factor for this process and is actually unrelated. Cerebral amyloid angiopathy typically occurs after the age of 55 years, has a prevalence as high as 10%–40% in this group, and occurs in up to 80% of patients with Alzheimer disease. Both genders are similarly affected.

Gross pathologic analysis can show lobar, corticosubcortical, and cortical hemorrhages of different ages and sizes, as well as signs of previous subarachnoid hemorrhage, all of these findings being the hallmark of this disease. Histologic analysis (eg, Congo red stain) reveals β-amyloid in the vessel walls and wall thinning and loosening, with luminal dilatation and perivascular inflammation. The vascular fragility explains the propensity to bleed, while the chronic hypoperfusion leads to leukoencephalopathy.

Peripheral micro- and macrohemorrhages, atraumatic convexal subarachnoid hemorrhage, superficial siderosis, and WMH are common radiologic manifestations (Fig 16) (49). Following the modified Boston criteria, the radiologic findings could suggest the diagnosis, but definitive

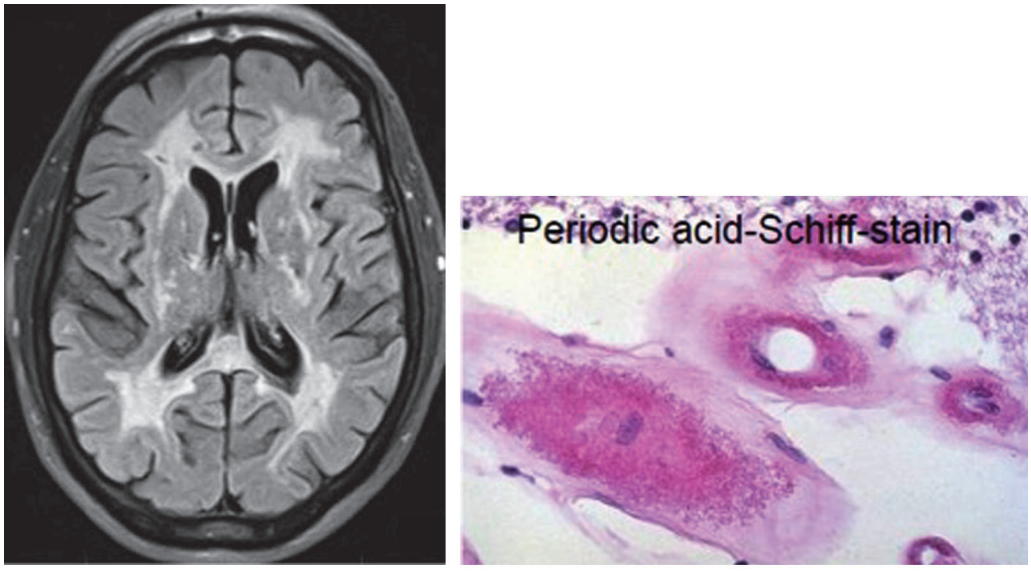

a. b.

Figure 17. CADASIL in a 65-year-old man. **(a)** Axial T2-weighted FLAIR image shows confluent periventricular WMHs, with typical involvement of the external capsules. (Courtesy of John H. Rees, MD, Partners Imaging Center, Sarasota, Fla.) **(b)** Photomicrograph shows thickening of the vessel walls, with deposition of granular material and narrowing of the lumen. (Periodic acid–Schiff stain.) (Courtesy of Alice Boyd Smith, MD, Uniformed Services University of the Health Sciences, Bethesda, Md.)

diagnosis of amyloid angiopathy requires postmortem examination (50,51).

Cerebral Autosomal-dominant Arteriopathy with Subcortical Infarcts and Leukoencephalopathy

CADASIL is an inherited nonarteriosclerotic and amyloid-negative small-vessel disease with autosomal-dominant transmission related to a mutation of the *NOTCH3* gene on chromosome 19. It has a prevalence of two to four per 100 000 and occurs with similar frequencies in both genders, with clinical onset typically in the 3rd and 4th decades. Common manifestations are migraines, recurrent ischemic strokes, and progressive cognitive impairment in young adults. CADASIL is the most frequent hereditary cause of subcortical vascular dementia. Pathologic analysis with electron microscopy reveals deposition of granular osmiophilic material around the vascular smooth muscles of small and medium-sized leptomeningeal arteries and long perforating arteries. This leads to loss of the normal smooth muscle cells, which leads to narrowing and obliteration of the small-vessel lumen (52–54).

The radiologic findings follow a characteristic course. First, until the end of the 3rd decade, most patients present with WMHs in the temporal pole, which is a differentiating feature from other microvascular diseases. In the 4th decade, the WMHs progress to the posterior temporal, frontal, and parietal regions, as well as the basal nuclei and thalami. Subcortical U-fibers can be involved, and subcortical lacunar infarcts become a common finding. Involvement of the external capsule and corpus callosum, which are other important markers for CADASIL, can also be observed. Lastly, in the 5th decade, microbleeds develop, and consequently, at age 50–60 years, extensive WMHs, lacunes, and microbleeds are often present (Fig 17). Angiography should be avoided if possible, due to the high risk of complications (54).

Table 2 shows differentiating features between CADASIL, small-vessel disease related to arteriolosclerosis, and autoimmune white matter diseases.

Primary Angiitis of the Central Nervous System

PACNS is a rare idiopathic vasculitis limited to the brain and spinal cord. It has been most frequently observed in the 5th and 6th decades of life, with similar frequency in both sexes. The history is nonspecific; headache and encephalopathy are common manifestations, while stroke and hemorrhage can occasionally be seen. Laboratory findings may show elevated inflammatory markers and a high protein level in cerebrospinal fluid.

Pathologically, PACNS consists of inflammation, intimal proliferation, and occlusion and necrosis of the small and medium-sized arteries, frequently involving the leptomeningeal and cortical vessels (Fig 18). Although the radiologic findings are nonspecific, MR imaging is virtually always abnormal, meaning that a normal MR imaging study could help rule out PACNS. Common reported manifes-

Table 2: Common Findings in CADASIL, SVD Related to Age and Risk Factors, MS, NMO, and ADEM

Findings or Locations	CADASIL	SVD-Arteriolosclerosis	MS	NMO	ADEM
Clinical course	Progressive	Progressive	Multiphasic	Recurrent (~90%)	Monophasic (~90%)
Histologic	Granular osmiophilic material around vascular smooth muscle	Arteriolosclerosis, lipohyalinosis, fibrinoid necrosis	Perivenular (Dawson fingers)	Not perivenular	Perivenular
Periventricular	Yes, including external capsule	Yes Symmetric Less likely to abut ependyma	Yes Asymmetric More likely to abut ependyma	Yes, usually later in disease course Around third to fourth ventricles	Yes, larger lesions
Temporal pole	Yes, typical and early	Uncommon	Yes	Uncommon	Sometimes
Corpus callosum lesions	Common (up to 40%)	Uncommon	Very common	Common	Uncommon
U-fibers	Yes	No	Yes	No	Yes
Cortex	Uncommon	Uncommon	Yes	No	Yes
Basal nuclei	Yes	Yes	Uncommon	Uncommon	Yes
Optic nerve	No	No	Yes	Yes	Uncommon
Brainstem	Uncommon until late	Pons, central	Pons, peripheral Dorsal and ventral Asymmetric Well-defined	Medulla oblongata Dorsal Asymmetric Poorly defined	Midbrain and pons Ventral Bilateral and symmetric Poorly defined
Spine	No	No	Focal, peripheral, posterior, and lateral Short segment	Longitudinal myelitis	Confluent Longitudinal myelitis
Laboratory	Genetic analysis: mutation of *NOTCH3* gene on chromosome 19	Vascular risk factors (eg, hypertension, diabetes, migraines)	Oligoclonal bands (up to 90%) High IgG (CSF) Myelin basic protein	NMO-IgG (50%–90%) CSF pleocytosis	CSF pleocytosis Anti-MOG IgG

Note.—CSF = cerebrospinal fluid, IgG = immunoglobulin G, MOG = myelin oligodendrocyte glycoprotein, SVD = small-vessel disease.

tations include multiple cortical-subcortical infarcts, hemorrhages, and parenchymal and leptomeningeal enhancement. Conventional angiography can sometimes demonstrate multifocal narrowing of the small and medium-sized vessels, but brain biopsy may be required to confirm the diagnosis (55,56).

Susac Syndrome

This is a rare but underdiagnosed small-vessel disease that occurs in young adults (20–40 years), more common in women (2:1). Susac syndrome seems to be a form of vasculitis produced by antiendothelial antibodies to specific neural vessels. The immune attack results in endotheliopathy that involves the cochlea, retina, and brain, with consequent microinfarcts in these locations, explaining the clinical triad of the disease: hearing loss (sensorineural), visual loss, and encephalopathy. Ophthalmoscopy is a cornerstone of the diagnosis, demonstrating characteristic findings such as branch retinal artery occlusion with retinal infarcts, arterial hyperfluorescence, and leakage of fluorescein. Pathologically, damaged endothelial cells, thrombus formation, vascular occlusion, and vascular wall leakage have been described.

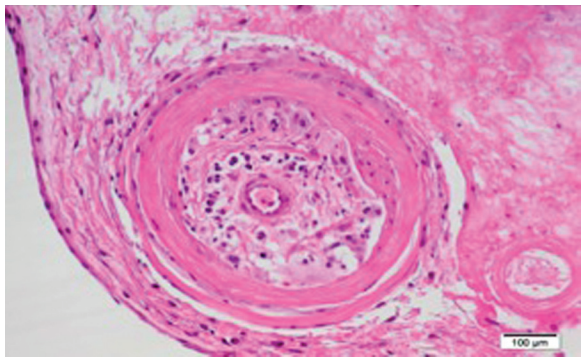

Figure 18. PACNS. Photomicrograph shows a hyalinized vessel wall, granulomatous inflammation with multinucleated giant cells both inside and outside the vessel, and a small residual lumen; the adjacent brain parenchyma was necrotic. (Hematoxylin-eosin stain; original magnification, ×200.)

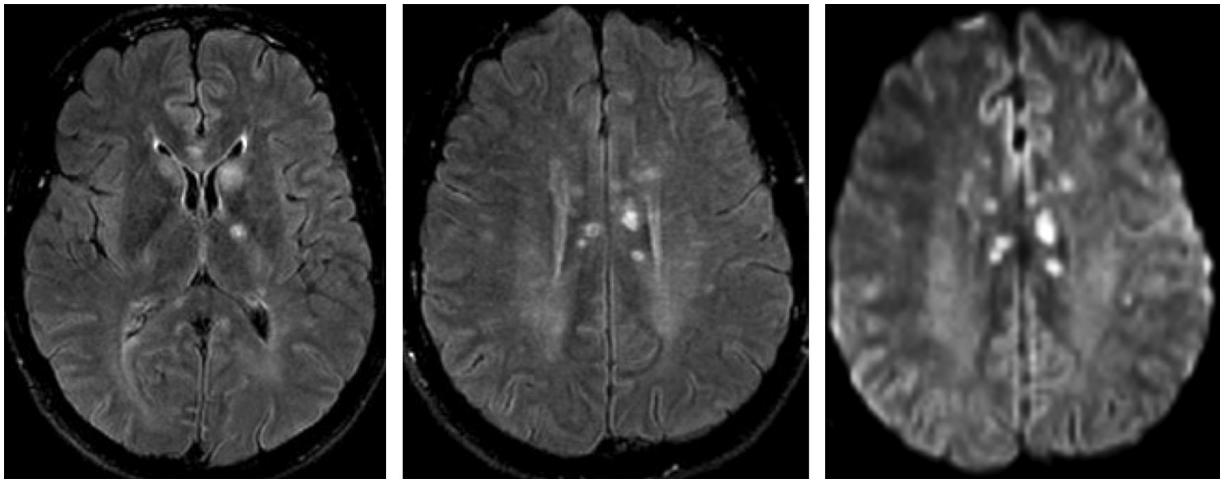

a. **b.** **c.**

Figure 19. Susac syndrome in a 23-year-old man. Axial T2-weighted FLAIR images show hyperintense lesions involving the periventricular white and deep gray matter **(a)** and corpus callosum **(b)**, with restricted diffusion on the diffusion-weighted image **(c)**.

MR imaging shows multiple microinfarcts in different phases of evolution, some of them with diffusion restriction and contrast enhancement. Leptomeningeal enhancement can be seen in one-third of patients, while parenchymal enhancement can be seen in two-thirds. Corpus callosum involvement is the rule. The central region of the corpus callosum is more frequently affected, rather than the callososeptal interface, and the lesions are classically described as "snowball" and can extend to involve the entire thickness of the callosum (Fig 19). Some lesions are cerebrospinal fluid isointense and are more hypointense on T1-weighted images ("black holes"), reflecting more severe damage, which could lead to chronic atrophy of the corpus callosum (57–59).

Systemic Lupus Erythematosus

SLE is a vasculopathy combining several pathogenic mechanisms. Up to 50% of patients with lupus develop neuropsychiatric SLE (NPSLE), which represents a major diagnostic challenge, a main cause of morbidity, and the cause of death in approximately 19% of patients with SLE. Vascular disease is the hallmark of NPSLE. At the onset of symptomatic NPSLE, and at a mean age of 41 years, small-vessel disease is already present in more than 50% of patients, large-vessel strokes in 13%, and inflammatory-type lesions in 6.5% (Fig 20) (60). Prospective large studies analyzing brain MR images, autopsy specimens, and histopathologic findings in NPSLE have shown correlation between MR imaging lesions and pathologic evidence of accelerated arteriolosclerosis (type 1 small-vessel disease) as well as immune-mediated vasculopathy (type 4 small-vessel disease) (61).

Toxic-Metabolic White Matter Diseases

Osmotic Myelinolysis

Osmotic myelinolysis occurs with osmotic stress, most often the rapid correction of hyponatremia, especially in the context of alcohol abuse or anorexia. Disorientation, vomiting, spastic quadriplegia, unresponsiveness, and cranial nerve palsies are classic symptoms. Histologic analysis reveals edema and demyelination, sparing the

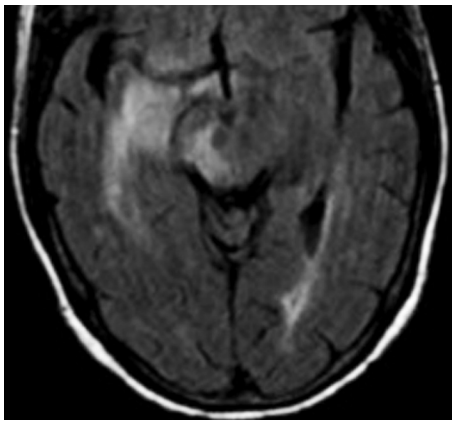

Figure 20. Neuropsychiatric lupus in a 36-year-old woman. Axial T2-weighted FLAIR image shows extensive hyperintensity involving white and gray matter of the right anterior temporal lobe and right midbrain. Small foci of contrast enhancement and restricted diffusion were also present.

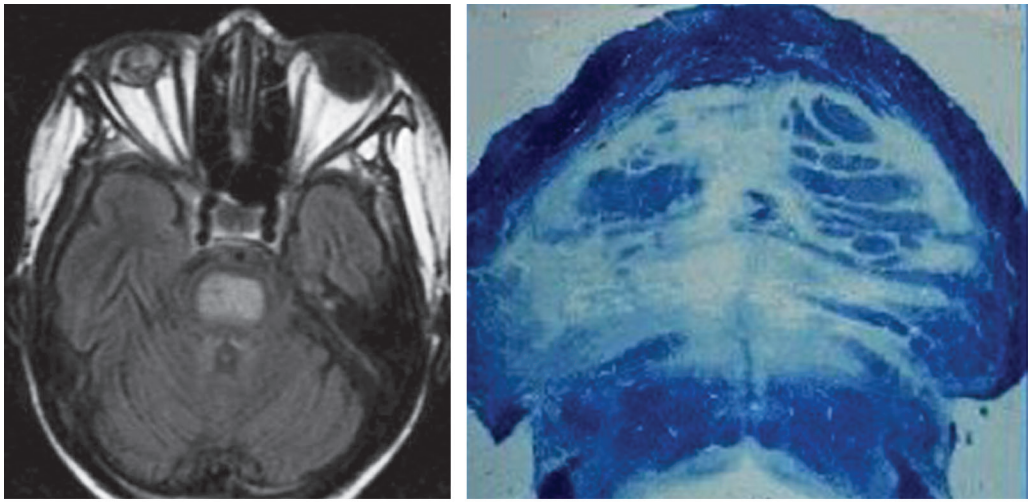

a. **b.**

Figure 21. Osmotic myelinolysis after rapid hyponatremia correction in a 67-year-old man. **(a)** Axial T2-weighted FLAIR image shows extensive central pontine hyperintensity sparing the periphery. **(b)** Gross specimen shows severe demyelination (white areas) sparing the peripheral part of the pons and the descending corticospinal tracts. (Luxol fast blue stain.)

blood vessels and frequently the long tracts (eg, corticospinal). In 65% of cases, it involves the pons and is typically central with sparing of the periphery. In other cases, it involves the thalami, basal nuclei, and subcortical white matter (Fig 21). In the acute phase, diffusion restriction can be present (62).

Treatment-related Leukoencephalopathies

Many therapies are associated with brain changes. More commonly recognized are those associated with methotrexate, several chemotherapies (fluorouracil, cytarabine), and antiepileptics (vigabatrin).

Methotrexate Leukoencephalopathy.—This is related to high doses of methotrexate, usually in the setting of hematologic malignancies, uncommon in rheumatologic diseases where the doses are lower. Typically this entity involves the frontoparietal white matter and centrum semiovale in small regions, but sometimes it can demonstrate extensive diffuse involvement of periventricular and deep white matter. It commonly shows no contrast enhancement or mass effect (Fig 22) (63).

Posterior Reversible Encephalopathy Syndrome

Posterior reversible encephalopathy syndrome (PRES) occurs as a result of a dysfunction in cerebrovascular regulation, which may be induced by hypertensive crisis, preeclampsia/eclampsia, or cytotoxic drugs. PRES typically involves the cortical and subcortical white matter areas. Radiologically, it is characterized by bilateral areas of T2 hyperintense edema, more frequently involving the parieto-occipital and posterior frontal regions (Fig 23). Although generally reversible with rapid treatment, PRES may be complicated by infarcts or hemorrhages. MR imaging can be performed to support the diagnosis, exclude other acute findings, and evaluate for complications (64).

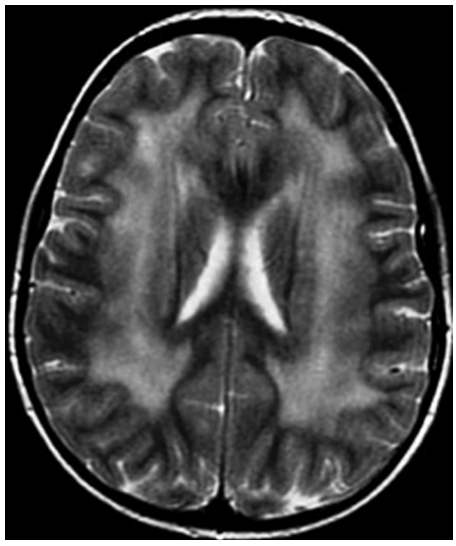

Figure 22. Methotrexate leukoencephalopathy in a 7-year-old boy due to high doses of chemotherapy for lymphoblastic leukemia. Axial T2-weighted image shows an extreme case with extensive areas of high signal intensity involving the bilateral periventricular and deep white matter, without mass effect or atrophy.

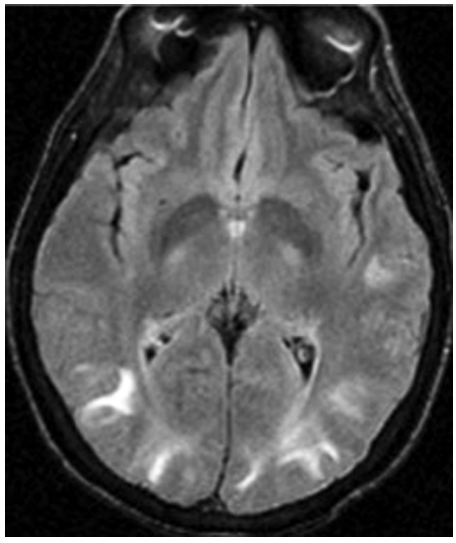

Figure 23. PRES in a 28-year-old woman in the setting of preeclampsia. Axial T2-weighted FLAIR image shows subcortical edematous areas involving the bilateral occipital regions.

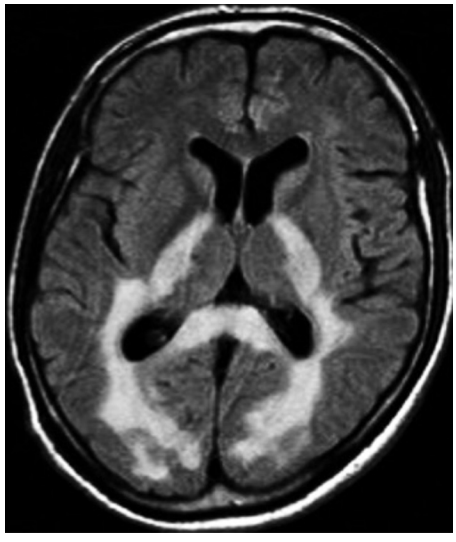

Figure 24. Heroin-induced leukoencephalopathy in a 26-year-old man. Axial T2-weighted FLAIR image shows bilateral extensive involvement of posterior white matter, the posterior arms of the internal capsule, and the splenium of the corpus callosum.

Ethanol-related Diseases

Wernicke Encephalopathy.—The mechanism is related to the thiamine (vitamin B1) deficiency, which is responsible for the deficit in production of some key enzymes for the Krebs energy cycle. Classic symptoms includes ataxia, nystagmus, ophthalmoplegia, and severe memory impairment. Typical locations are the mammillary bodies, periaqueductal gray matter, medial thalami, and tectal plate, with signal intensity anomaly preceding atrophic changes.

Marchiafava-Bignami Disease.—Chronic alcoholism with consumption of large amounts of alcohol is responsible for this entity. Confusion and seizures are the classic presentation. Marchiafava-Bignami disease preferentially involves the middle layers of the body of the corpus callosum, although any part of it may be affected. There are two forms described: type A, with extensive lesions, swelling of the corpus callosum, and poor outcome; and type B, with smaller lesions, without callosal swelling, with better outcome. Other white matter connection tracts and the cortex can also be involved. Diffusion restriction of the corpus callosum in the acute phase has been recognized (Fig 3c) (65).

Illicit Drugs: Heroin Inhalation

This is produced by inhalation of the vapors that result from heating the heroin ("chasing the dragon"). Extrapyramidal and cerebellar syndromes are typical. Histologic analysis shows spongiform degeneration of the affected regions. Commonly involved are the posterior white matter, internal capsule, brainstem, and cerebellar peduncles (Fig 24) (66).

Delayed Hypoxic Ischemic Injury

This could occur from different reasons, some of the most common being poisoning and recovery after cardiac arrest.

Carbon Monoxide Leukoencephalopathy

This is the most common type of unintentional poisoning in North America. The mechanism of hypoxia is directly related to the affinity of carbon

Table 3: Summary of White Matter Diseases

Disease	Description*
MS	Dawson fingers, dissemination in space (periventricular, juxtacortical, brainstem, spinal cord) and in time (single MR imaging study: both contrast-enhancing and nonenhancing lesions; follow-up MR imaging: new lesions)
TDL	Tumefactive MS, may show open-ring enhancement and restricted diffusion—open to gray matter or ventricular surface, variable mass effect
NMO	Autoimmunity to aquaporin-4; triad of optic neuritis, transverse myelitis, and NMO-IgG
ADEM	Multiple rounded lesions, bigger than in MS, more involvement of gray matter than in MS, transverse myelitis in one-third of cases
Differential diagnosis of ring-enhancing lesions	MAGIC DR: *m*etastasis, *a*bscess, *g*lioblastoma, *i*nfarct (subacute), *c*ontusion (subacute), *d*emyelination (MS-like), *r*adiation (necrosis)
Lyme disease	Neuroborreliosis, CNS involvement in 10%–15%, WMH plus leptomeningeal or cranial nerve enhancement
PML	JC virus, peripheral geographic areas, no atrophy (differential diagnosis: HIV encephalopathy), no significant mass effect or enhancement (except in setting of IRIS and natalizumab)
HIV encephalopathy	Central or periventricular white matter, cerebral atrophy
Amyloid angiopathy	Peripheral (micro)bleeds, superficial siderosis, WMH
CADASIL	Temporal poles, external capsule, multiple lacunar infarcts
PACNS	Abnormal MR imaging; a normal MR imaging study makes PACNS unlikely
Susac syndrome	"E" syndrome: mechanism, endotheliopathy; clinical triad of ear problems (hearing loss), eye problems (visual loss), and encephalopathy; callosal "snowball"; internal capsule "string of pearls"
Osmotic myelinolysis	Two-thirds of cases are pontine (central, sparing the periphery); one-third are supratentorial
Methotrexate leukoencephalopathy	Periventricular leukoencephalopathy, no enhancement or mass effect
PRES	Posterior > anterior circulation, subcortical

*CNS = central nervous system, IgG = immunoglobulin G, IRIS = immune reconstitution inflammatory syndrome.

monoxide for hemoglobin, about 200 times greater than that of oxygen. The globi pallidi are typically involved, but periventricular white matter injury can be a delayed manifestation (66).

Radiation Leukoencephalopathy

This may occur in up to one-third of patients and is usually related to whole-brain radiation therapy and/or high doses (30–40 Gy). Most often, patients have additional risk factors: large target areas and associated treatments (chemotherapy). It frequently occurs months and even years after the radiation therapy. More severe damage could show necrotic changes with contrast enhancement. Radiation injury may also cause mineralizing microangiopathy with extensive calcifications (67,68).

Table 3 provides a summary of the main features of white matter diseases.

Conclusion

A systematic approach combining imaging, clinical, and laboratory data is crucial for making the correct diagnosis in white matter disorders. Understanding the pathologic substrate is fundamental for understanding the radiologic manifestations.

Acknowledgments.—We thank Jacqueline A. Bello, MD, Steven J. Goldstein, MD, John H. Rees, MD, Robert E. Schmidt, MD, PhD, and Alice Boyd Smith, MD, for providing images.

References

1. Smith AB, Smirniotopoulos JG. Imaging evaluation of demyelinating processes of the central nervous system. Postgrad Med J 2010;86(1014):218–229.
2. Bakhti M, Aggarwal S, Simons M. Myelin architecture: zippering membranes tightly together. Cell Mol Life Sci 2014;71(7):1265–1277.
3. Paz Soldán MM, Pirko I. Biogenesis and significance of central nervous system myelin. Semin Neurol 2012;32(1):9–14.
4. Ragonese P, Aridon P, Salemi G, D'Amelio M, Savettieri G. Mortality in multiple sclerosis: a review. Eur J Neurol 2008;15(2):123–127.
5. Karussis D. The diagnosis of multiple sclerosis and the various related demyelinating syndromes: a critical review. J Autoimmun 2014;48-49:134–142.
6. Okuda DT. Unanticipated demyelinating pathology of the CNS. Nat Rev Neurol 2009;5(11):591–597.
7. Williams R, Buchheit CL, Berman NEJ, LeVine SM. Pathogenic implications of iron accumulation in multiple sclerosis. J Neurochem 2012;120(1):7–25.
8. Filippi M, Evangelou N, Kangarlu A, et al. Ultra-high-field MR imaging in multiple sclerosis. J Neurol Neurosurg Psychiatry 2014;85(1):60–66.

9. Polman CH, Reingold SC, Banwell B, et al. Diagnostic criteria for multiple sclerosis: 2010 revisions to the McDonald criteria. Ann Neurol 2011;69(2):292–302.
10. Montalban X, Tintoré M, Swanton J, et al. MRI criteria for MS in patients with clinically isolated syndromes. Neurology 2010;74(5):427–434.
11. Cotton F, Weiner HL, Jolesz FA, Guttmann CRG. MRI contrast uptake in new lesions in relapsing-remitting MS followed at weekly intervals. Neurology 2003;60(4):640–646.
12. Tallantyre EC, Morgan PS, Dixon JE, et al. A comparison of 3T and 7T in the detection of small parenchymal veins within MS lesions. Invest Radiol 2009;44(9):491–494.
13. Filippi M, Rocca MA. MR imaging of multiple sclerosis. Radiology 2011;259(3):659–681.
14. Grabner G, Dal-Bianco A, Schernthaner M, Vass K, Lassmann H, Trattnig S. Analysis of multiple sclerosis lesions using a fusion of 3.0 T FLAIR and 7.0 T SWI phase: FLAIR SWI. J Magn Reson Imaging 2011;33(3):543–549.
15. Lisanti CJ, Asbach P, Bradley WG Jr. The ependymal "dot-dash" sign: an MR imaging finding of early multiple sclerosis. AJNR Am J Neuroradiol 2005;26(8):2033–2036.
16. Roosendaal SD, Moraal B, Pouwels PJW, et al. Accumulation of cortical lesions in MS: relation with cognitive impairment. Mult Scler 2009;15(6):708–714.
17. Filippi M, Rocca MA, Calabrese M, et al. Intracortical lesions: relevance for new MRI diagnostic criteria for multiple sclerosis. Neurology 2010;75(22):1988–1994.
18. de Graaf WL, Kilsdonk ID, Lopez-Soriano A, et al. Clinical application of multi-contrast 7-T MR imaging in multiple sclerosis: increased lesion detection compared to 3 T confined to grey matter. Eur Radiol 2013;23(2):528–540.
19. Lu Z, Zhang B, Qiu W, et al. Comparative brain stem lesions on MRI of acute disseminated encephalomyelitis, neuromyelitis optica, and multiple sclerosis. PLoS One 2011;6(8):e22766.
20. Lycklama G, Thompson A, Filippi M, et al. Spinal-cord MRI in multiple sclerosis. Lancet Neurol 2003;2(9):555–562.
21. Solomon AJ, Klein EP, Bourdette D. "Undiagnosing" multiple sclerosis: the challenge of misdiagnosis in MS. Neurology 2012;78(24):1986–1991.
22. Al-Okaili RN, Krejza J, Wang S, Woo JH, Melhem ER. Advanced MR imaging techniques in the diagnosis of intraaxial brain tumors in adults. RadioGraphics 2006;26(suppl 1):S173–S189.
23. Cañellas AR, Gols AR, Izquierdo JR, Subirana MT, Gairin XM. Idiopathic inflammatory-demyelinating diseases of the central nervous system. Neuroradiology 2007;49(5):393–409.
24. Smirniotopoulos JG, Murphy FM, Rushing EJ, Rees JH, Schroeder JW. Patterns of contrast enhancement in the brain and meninges. RadioGraphics 2007;27(2):525–551.
25. Barnett Y, Sutton IJ, Ghadiri M, Masters L, Zivadinov R, Barnett MH. Conventional and advanced imaging in neuromyelitis optica. AJNR Am J Neuroradiol 2014;35(8):1458–1466.
26. Huh SY, Min JH, Kim W, et al. The usefulness of brain MRI at onset in the differentiation of multiple sclerosis and seropositive neuromyelitis optica spectrum disorders. Mult Scler 2014;20(6):695–704.
27. Rovira À, Sastre-Garriga J, Auger C, Rovira A. Idiopathic inflammatory demyelinating diseases of the brainstem. Semin Ultrasound CT MR 2013;34(2):123–130.
28. Sahraian MA, Radue EW, Minagar A. Neuromyelitis optica: clinical manifestations and neuroimaging features. Neurol Clin 2013;31(1):139–152.
29. Yonezu T, Ito S, Mori M, et al. "Bright spotty lesions" on spinal magnetic resonance imaging differentiate neuromyelitis optica from multiple sclerosis. Mult Scler 2014;20(3):331–337.
30. Kister I, Herbert J, Zhou Y, Ge Y. Ultrahigh-field MR (7 T) imaging of brain lesions in neuromyelitis optica. Mult Scler Int 2013;2013:398259.
31. Nakamura M, Misu T, Fujihara K, et al. Occurrence of acute large and edematous callosal lesions in neuromyelitis optica. Mult Scler 2009;15(6):695–700.
32. Tenembaum SN. Disseminated encephalomyelitis in children. Clin Neurol Neurosurg 2008;110(9):928–938.
33. DeSanto J, Ross JS. Spine infection/inflammation. Radiol Clin North Am 2011;49(1):105–127.
34. Smith AB, Smirniotopoulos JG, Rushing EJ. From the archives of the AFIP: central nervous system infections associated with human immunodeficiency virus infection—radiologic-pathologic correlation. RadioGraphics 2008;28(7):2033–2058.
35. Hildenbrand P, Craven DE, Jones R, Nemeskal P. Lyme neuroborreliosis: manifestations of a rapidly emerging zoonosis. AJNR Am J Neuroradiol 2009;30(6):1079–1087.
36. Wardlaw JM, Smith EE, Biessels GJ, et al. Neuroimaging standards for research into small vessel disease and its contribution to ageing and neurodegeneration. Lancet Neurol 2013;12(8):822–838.
37. Pantoni L. Cerebral small vessel disease: from pathogenesis and clinical characteristics to therapeutic challenges. Lancet Neurol 2010;9(7):689–701.
38. de Leeuw FE, de Groot JC, Achten E, et al. Prevalence of cerebral white matter lesions in elderly people: a population based magnetic resonance imaging study. The Rotterdam Scan Study. J Neurol Neurosurg Psychiatry 2001;70(1):9–14.
39. Fazekas F, Chawluk JB, Alavi A, Hurtig HI, Zimmerman RA. MR signal abnormalities at 1.5 T in Alzheimer's dementia and normal aging. AJR Am J Roentgenol 1987;149(2):351–356.
40. Wahlund LO, Barkhof F, Fazekas F, et al. A new rating scale for age-related white matter changes applicable to MRI and CT. Stroke 2001;32(6):1318–1322.
41. Duering M, Csanadi E, Gesierich B, et al. Incident lacunes preferentially localize to the edge of white matter hyperintensities: insights into the pathophysiology of cerebral small vessel disease. Brain 2013;136(Pt 9):2717–2726.
42. Erro ME, Gállego J, Herrera M, Bermejo B. Isolated pontine infarcts: etiopathogenic mechanisms. Eur J Neurol 2005;12(12):984–988.
43. Maillard P, Fletcher E, Harvey D, et al. White matter hyperintensity penumbra. Stroke 2011;42(7):1917–1922.
44. Schmidt R, Schmidt H, Haybaeck J, et al. Heterogeneity in age-related white matter changes. Acta Neuropathol (Berl) 2011;122(2):171–185.
45. Doubal FN, Dennis MS, Wardlaw JM. Characteristics of patients with minor ischaemic strokes and negative MRI: a cross-sectional study. J Neurol Neurosurg Psychiatry 2011;82(5):540–542.
46. Wardlaw JM, Smith C, Dichgans M. Mechanisms of sporadic cerebral small vessel disease: insights from neuroimaging. Lancet Neurol 2013;12(5):483–497.
47. Greenberg SM, Vernooij MW, Cordonnier C, et al. Cerebral microbleeds: a guide to detection and interpretation. Lancet Neurol 2009;8(2):165–174.
48. Scheltens P, Pasquier F, Weerts JG, Barkhof F, Leys D. Qualitative assessment of cerebral atrophy on MRI: inter- and intra-observer reproducibility in dementia and normal aging. Eur Neurol 1997;37(2):95–99.
49. Charidimou A, Gang Q, Werring DJ. Sporadic cerebral amyloid angiopathy revisited: recent insights into pathophysiology and clinical spectrum. J Neurol Neurosurg Psychiatry 2012;83(2):124–137.
50. Knudsen KA, Rosand J, Karluk D, Greenberg SM. Clinical diagnosis of cerebral amyloid angiopathy: validation of the Boston criteria. Neurology 2001;56(4):537–539.
51. Linn J, Halpin A, Demaerel P, et al. Prevalence of superficial siderosis in patients with cerebral amyloid angiopathy. Neurology 2010;74(17):1346–1350.
52. Chabriat H, Vahedi K, Iba-Zizen MT, et al. Clinical spectrum of CADASIL: a study of 7 families—cerebral autosomal dominant arteriopathy with subcortical infarcts and leukoencephalopathy. Lancet 1995;346(8980):934–939.
53. Singhal S, Rich P, Markus HS. The spatial distribution of MR imaging abnormalities in cerebral autosomal dominant arteriopathy with subcortical infarcts and leukoencephalopathy and their relationship to age and clinical features. AJNR Am J Neuroradiol 2005;26(10):2481–2487.
54. van den Boom R, Lesnik Oberstein SAJ, Ferrari MD, Haan J, van Buchem MA. Cerebral autosomal dominant arteriopathy with subcortical infarcts and leukoencephalopathy: MR imaging findings at different ages—3rd–6th decades. Radiology 2003;229(3):683–690.
55. Birnbaum J, Hellmann DB. Primary angiitis of the central nervous system. Arch Neurol 2009;66(6):704–709.

56. Abdel Razek AAK, Alvarez H, Bagg S, Refaat S, Castillo M. Imaging spectrum of CNS vasculitis. RadioGraphics 2014;34(4):873–894.
57. Susac JO, Hardman JM, Selhorst JB. Microangiopathy of the brain and retina. Neurology 1979;29(3):313–316.
58. Susac JO, Murtagh FR, Egan RA, et al. MRI findings in Susac's syndrome. Neurology 2003;61(12):1783–1787.
59. Kleffner I, Duning T, Lohmann H, et al. A brief review of Susac syndrome. J Neurol Sci 2012;322(1-2):35–40.
60. Sarbu N, Alobeidi F, Toledano P, et al. Brain abnormalities in newly diagnosed neuropsychiatric lupus: systematic MRI approach and correlation with clinical and laboratory data in a large multicenter cohort. Autoimmun Rev 2015;14(2):153–159.
61. Sibbitt WL Jr, Brooks WM, Kornfeld M, Hart BL, Bankhurst AD, Roldan C. Magnetic resonance imaging and brain histopathology in neuropsychiatric systemic lupus erythematosus. Semin Arthritis Rheum 2010;40(1):32–52. [Published correction appears in Semin Arthritis Rheum 2011;40(4):369.]
62. Singh TD, Fugate JE, Rabinstein AA. Central pontine and extrapontine myelinolysis: a systematic review. Eur J Neurol 2014;21(12):1443–1450.
63. Reddick WE, Glass JO, Helton KJ, et al. Prevalence of leukoencephalopathy in children treated for acute lymphoblastic leukemia with high-dose methotrexate. AJNR Am J Neuroradiol 2005;26(5):1263–1269.
64. Fugate JE, Rabinstein AA. Posterior reversible encephalopathy syndrome: clinical and radiological manifestations, pathophysiology, and outstanding questions. Lancet Neurol 2015;14(9):914–925.
65. Johkura K, Naito M, Naka T. Cortical involvement in Marchiafava-Bignami disease. AJNR Am J Neuroradiol 2005;26(3):670–673.
66. Tormoehlen LM. Toxic leukoencephalopathies. Neurol Clin 2011;29(3):591–605.
67. Rimkus CdeM, Andrade CS, Leite CdaC, McKinney AM, Lucato LT. Toxic leukoencephalopathies, including drug, medication, environmental, and radiation-induced encephalopathic syndromes. Semin Ultrasound CT MR 2014;35(2):97–117.
68. Cummings M, Dougherty DW, Mohile NA, Walter KA, Usuki KY, Milano MT. Severe radiation-induced leukoencephalopathy: case report and literature review. Adv Radiat Oncol 2016;1(1):17–20.